Moussa, FB.; Kutner, W.; Beduk, T.; Sena-Torralba, A.; Mostafavi, E. (2024). Electrochemical bio- and chemosensors for cancer biomarkers: Natural (with antibodies) versus biomimicking artificial (with aptamers and molecularly imprinted polymers) recognition. Talanta. 267. https://doi.org/10.1016/j.talanta.2023.125259

Electrochemical bio- and chemosensors for cancer biomarkers: Natural (with antibodies) versus biomimicking artificial (with aptamers and molecularly imprinted polymers) recognition

Fatah Ben Moussa[a], Wlodzimierz Kutner[b,c], Tutku Beduk[d], Amadeo Sena-Torralba[e], and Ebrahim Mostafavi[f,g]

[a] *Process Engineering Laboratory, Applied Sciences Faculty, Kasdi Merbah University, Ouargla, 30000, Algeria.*

[b] *Institute of Physical Chemistry, Polish Academy of Sciences, Kasprzaka 44/52, 01-224 Warsaw, Poland.*

[c] *Faculty of Mathematics and Natural Sciences. School of Sciences, Cardinal Stefan Wyszynski University in Warsaw, Wóycickiego 1/3, 01-815 Warsaw, Poland.*

[d] *Silicon Austria Labs GmbH: Sensor Systems, Europastrasse 12, 9524 Villach, Austria.*

[e] *Instituto Interuniversitario de Investigación de Reconocimiento Molecular y Desarrollo Tecnológico (IDM), Universitat Politècnica de València, Universitat de València, Camino de Vera s/n, 46022 Valencia, Spain.*

[f] *Department of Medicine, Stanford University School of Medicine, Stanford, CA, 94305, USA.*

[g] *Stanford Cardiovascular Institute, Stanford University School of Medicine, Stanford, CA, 94305, USA.*

Corresponding author e-mail address: benmoussa.fatah@univ-ouargla.dz

Full postal address: Cité 18 février, N4, Adrar, 01000, Algeria.

Abstract

Electrochemical (EC) bio- and chemosensors are highly promising for on-chip and point-of-care testing (POST) devices. They can make a breakthrough in early cancer diagnosis. Most current EC sensors for cancer biomarkers' detection and determination use natural antibodies as recognition units. However, those quickly lose their biorecognition ability upon exposure to harsh environments, comprising extreme pH, humidity, temperature, etc. So-called "plastic antibodies," including aptamers and molecularly imprinted polymers (MIPs), are hypothesized to be a smart alternative to antibodies. They have attracted the interest of the sensor research community, offering a low cost-to-performance ratio with high stability, an essential advantage toward their commercialization. Herein, we critically review recent technological advances in devising and fabricating EC bio- and chemosensors for cancer biomarkers, classifying them according to the type of recognition unit used into three categories, i.e., antibody-, aptamer-, and MIP-based EC sensors for cancer biomarkers. Each sensor fabrication strategy has been discussed, from the devising concept to cancer sensing applications, including using different innovative nanomaterials and signal transduction strategies. Moreover, employing each recognition unit in the EC sensing of cancer biomarkers has been critically compared in detail to enlighten each recognition unit's advantages, effectiveness, and limitations.

Keywords: Electrochemical detection; cancer biomarker; antibody; aptamer; MIP.

List of Abbreviations

AAM	Acrylamide
Ab1	Primary antibody
Ab2	Secondary antibody
AFP	α-fetoprotein
AgNP	Silver nanoparticle
Ag-SPE	Screen-printed silver electrode
AIBN	Azobisisobutyronitrile
AMNFs	Antimonene
AOT	8-Amino-1-octanethiol
APS	Ammonium persulfate
Apt1	Primary aptamer
Apt2	Secondary aptamer
ATA	Poly(2-amino terephthalic acid)
AuE	Gold electrode
AuNP	Gold nanoparticle
Au-SPE	Screen-printed gold electrode
BRCA1	Breast cancer gene 1
BSA	Bovine serum albumin
CA 125	Cancer antigen 125
CA 15-3	Cancer anitgen15–3
CA 19-9	Cancer antigen 19-9
CBMA	Carboxybetaine methacrylate
CD45	Cluster of differentiation 45
CD44	Cluster of differentiation 44
CD56	Cluster of differentiation 56
cDNA	Complementary DNA
CEA	Carcinoembryonic antigen
CEACAM5	Carcinoembryonic antigen cell adhesion molecule 5
CS	Chitosan
C-SPE	Screen-printed carbon electrode
CNT-CPE	Carbon-nanotube carbon paste electrode
CV	Cyclic voltammetry
Cys-VIMBF4	1-[3-(*N*-cystamine)propyl]-3-vinylimidazolium tetrafluoroborate ionic liquid
DNA(C1)	Complementary DNA 1
DPASV	Differential pulse anodic stripping voltammetry
DPV	Differential pulse voltammetry
dsDNA	Double-stranded DNA
DSP	3,3′-Dithiodipropionic acid di(*N*-hydroxysuccinimide ester)
EDC	Ethyl-3-(-3-dimethylaminopropyl)
EGDMA	Ethylene glycol dimethacrylate
EGFR	Epidermal growth factor receptor
EIS	Electrochemical impedance spectroscopy
ELISA	Enzyme-linked immunoassay
EpCAM	Epithelial cell adhesion molecule
ER	Estrogen receptor
Fc-g-PLL	Ferrocene-grafted-polylysine
FTO	Fluorine-doped tin oxide (electrode)
GA	Glutaraldehyde
G-Au	Glutathione-capped gold
GCE	Glassy carbon electrode
GNP	Graphene nanoplatelet
GP	Graphene-poly(3-aminobenzoic acid) (GP-P3ABA)
GO	Graphene oxide
GQD	Graphene quantum dot
GR	Graphene
G-SPE	Screen-printed graphite electrode
HA	Hyaluronic acid
hCG	Human chorionic gonadotropin
HE4	Human epididymis protein 4
hemin-G4	Hemin-G-quadruplex
HER2/NEU	Human epidermal growth factor receptor 2
HNF-AuNP	Hybrid nanoflower linked to a gold nanoparticle
HRP	Horseradish peroxidase
HSA	Human serum albumin
ITO	Indium-tin oxide
LA	Lactic acid
LOD	Limit of detection
LOQ	Limit of quantification
LPA	Lipoic acid *N*-hydroxysuccinimide ester
LSV	Linear sweep voltammetry
MAA	Methacrylic acid
MB	Methylene blue
MB	Magnetic bead
MIP	Molecularly imprinted polymer
MOF	Metal-organic framework
MPBA	4-Mercaptophenylboronic acid
MSA	Mercaptosuccinic acid
MWCNT	Multi-walled carbon nanotube
NB	Neutral Red
NC	Nanocrystal
NF	Nanoflower
NG	Nitrogen-doped graphene
NHS	*N*-hydroxysuccinimide
NIPAm	*N*-isopropylacrylamide
NiHCF	Nickel hexacyanoferrate
NNMBA	*N*,*N*′-methylenebisacrylamide
NPV	Normal pulse voltammetry
NSE	Neuron specific-enolase
NuMA Or NMP22	Nuclear mitotic apparatus protein
PA	Pyruvic acid
PANI	Polyaniline
PBNP	Prussian Blue nanoparticle
PDDA	Poly(diallyldimethylammonium chloride)
PEDOT	Poly(3,4-ethylenedioxythiophene)
PEP	Polypeptide
PGE	Pencil graphite electrode
PGMA	Poly(glycidyl methacrylate)
PHSGNP	Porous-hollowed-silver-gold core-shell nanoparticle
PMB	Poly(methylene blue)
POCT	Point-of-care testing
Poly(3-HPA)	Poly(3-hydroxypropanoic acid)
PolyCBMA	Poly(carboxybetaine methacrylate)
PSA	Prostate-specific antigen
PTB	Poly(Toluidine Blue)
Pth	Polythionine
Pthi	Polythiophene
QD	Quantum dot
rGO	Reduced graphene oxide
RhB	Rhodamine B
SCE	Saturated calomel electrode
ssDNA	Single-stranded DNA
Strp	Streptavidin
SWCNT	Single-walled carbon nanotube
SWV	Square wave voltammetry
T-GO	Thiolated graphene oxide
TB	Toluidine Blue
Thi	Thiophene
TNP	Triangle nanoparticle
TRIM	Trimethylolpropane trimethacrylate
VA-MWCNT	Vertically aligned multi-walled carbon nanotube
VG	Vertical graphene
WHO	World Health Organization
YNC	Yolk-shell nanocrystal

Introduction

According to the World Health Organization (WHO), there were ~10 million fatalities from cancer by 2021 [1], making it a leading cause of death worldwide. Early cancer diagnosis and staging are crucial for effective treatment and high chances of survival [2]. Cancer diagnosis still relies on medical imaging techniques, including magnetic resonance imaging (MRI), computer-assisted tomography (CAT), mammography, X-ray imaging, histopathology, and cytology. However, those tools sometimes lack sensitivity, especially in the early stages of cancer [3] [4].

A biomarker (short for "biological marker"), an indicator of normal biological processes in tissue or body fluid, objectively measures and evaluates pathogenic processes or responses to pharmacological therapeutic interventions. Cancer biomarkers include proteins, carbohydrates, nucleic acids, and peptides (Table 1). Another category, called metabolite-based cancer biomarkers, expresses a precise signature related to malignant cell formation [5]. The cancer biomarker level expressing an abnormal cancer activity can be a breakthrough in cancer's early diagnosis and development prognosis.

In the last decade, the interest in sensors for cancer biomarkers has risen because of the need for rapid, sensitive, and precise analytical devices quantifying these biomarkers. Those sensors fall into the optical [6,7], microgravimetric [8], and thermometric [9] main categories depending on the signal transduction method employed. Although efficient, those methods often suffer from several operational drawbacks [10], e.g., being quite expensive or requiring sophisticated equipment. Moreover, they need an expert to operate and require obeying rigorous sample preparation procedures. Another category involves electrochemical, prevailingly potentiometric, amperometric, conductimetric, capacitive, and impedimetric sensors, which have gained much attention in bio-compounds determination, holding promise to overcome the above limitations. EC sensors for cancer biomarkers are a strong candidates for clinical monitoring of cancer diseases with their advantages, involving fast response (within seconds), high sensitivity and detectability, low sample consumption, and cost-effectiveness.

The recognition unit, crucial to any sensor, including the EC sensor, can be either natural, i.e., biological, or artificial, i.e., synthetic. Depending on the nature of this unit, IUPAC classifies the former as biosensors [11] and the latter as chemosensors [12]. Accordingly, antibodies-featuring

EC sensors are considered biosensors or immunosensors, to be more precise, while those containing aptamers or MIPs are considered chemosensors. EC immunosensors' role in cancer biomarkers in clinical analysis has recently increased [13]. Sensor devising concerning the type of recognition unit used and the method of its surface immobilization, as well as the transduction nature, have substantially been developed [14] [15] [16].

Cancer biomarker electrochemical sensing encompasses various strategies, including those engaging antibodies, aptamers, and molecularly imprinted polymers (MIPs). Each of these strategies employs a unique detection mechanism. Antibody-based sensing involves immobilizing target biomarkers on the electrode surface by functionalizing electrodes with antibodies that specifically bind them. Following the antibody-antigen interaction, changes in impedance or current are measured to determine biomarkers. This sensing supports both label-free and sandwich modes. The label-free mode allows real-time monitoring of direct antibody-biomarker interactions [17], whereas the sandwich mode uses dual antibody binding to increase sensitivity [18]. Aptamers are attached to electrodes in aptamer-based sensing to selectively bind target biomolecules, causing conformational changes in the aptamers and modulating electrochemical signals. Aptamer-based methods can adopt label-free [19] or sandwich modes [20]. MIPs are integrated into sensors by modifying the electrodes with MIPs bearing molecular cavities, selectively binding molecules of target biomarkers. When these cavities bind, their structural properties change, influencing their electrochemical behavior and allowing for sensitive detection [21]. All the above strategies combine molecular recognition with electrochemical transduction, propelling cancer biomarker detection forward by amplifying signals and ensuring versatile and precise determination.

The recognition unit nature can directly affect several important analytical sensor parameters, e.g., selectivity and stability. In the literature, only three types of recognition units were reported in designing an EC cancer biomarker sensor. Those can be classified into two main categories. One involves natural antibodies. The other embraces "plastic antibodies," which include aptamers and MIPs. To date, various reviews have partially focused on incorporating nanomaterials with antibodies and aptamers for signal enhancement in the EC sensing of cancer markers [22] [23] [24] [25] and others on using MIPs for cancer diagnosing [21]. However, none of these reviews have classified and compared these natural and biomimetics recognition units against each other, which is the main focus of the present review article.

Herein, we report on the recent advances in fabricating EC sensors for cancer biomarkers, classifying them based on the type of recognition unit used into three categories: vis., the antibody, aptamer, and MIP-based EC sensors. Each sensor fabrication strategy has been discussed, from the design concept to cancer sensing application, including using different innovative nanomaterials and signal amplification strategies. Moreover, a detailed comparison of the use of each recognition unit in the EC sensing application of cancer biomarkers has been reported to enlighten each receptor's advantages, effectiveness, and limitations.

Table 1. Selected cancer biomarkers and their properties.

Biomarker	**Biomarker nature**	**Cancer location**	**Specimen**	**Clinical use**
α-fetoprotein (AFP)	Protein	Testicular	Serum/plasma	Managing of cancer
Cancer antigen 15- 3 (CA 15-3)	Protein	Breast	Serum/plasma	Monitoring of disease; response to therapy
Cancer antigen 19-9 (CA 19-9)	Protein	Pancreatic	Serum/plasma	Monitoring of disease
Cancer antigen 125 (CA 125)	Protein	Ovarian	Serum/plasma	Monitoring of disease; response to therapy
Carcinoembryonic antigen (CEA)	Protein	Colon	Serum/plasma	Monitoring of disease; response to therapy
EpCAM, CD45, cytokeratins8, 18+,19+	Protein	Breast	Whole blood	Monitoring of progression and survival
Epidermal growth factor receptor (EGFR)	Protein	Colon	Tissue	Therapy selection
HER2/NEU	Protein	Breast	Serum; tissue	Monitoring of progression; therapy selection
Human chorionic gonadotropin (hCG)	Protein	Testicular	Serum	Staging of cancer
Human epididymis protein 4 (HE4)	Protein	Ovarian	Serum	Monitoring of progression and recurrence
prostate-specific antigen (PSA)	Protein	Prostate	Serum	Screening for disease
Nuclear mitotic apparatus protein (NMP22)	Protein	Bladder	Urine	Diagnosis and monitoring of disease
CD44	Protein	Gastric colon	Serum	Diagnosis
CEACAM5 (DNA)	DNA	Colon	Serum/plasma	Monitoring of disease; response to therapy
BRCA1 (DNA)	DNA	Breast, ovarian	Serum	Diagnosis
Sarcosine	Metabolite	Prostate	Serum/urine	Diagnosis and monitoring of disease
CD56	Protein	Lung	Serum/plasma	Diagnosis
Neuron specific-enolase (NSE)	Protein	Lung, pancreatic, thyroid	Serum	Monitoring of disease
Pyruvic acid	Metabolite	Cancer cells	Serum urine	Diagnosis and monitoring of disease
Lactic acid	Metabolite	Cancer cells	Serum urine	Diagnosis and monitoring of disease

Electrochemical antibody-based sensors for cancer biomarkers

Antibodies are large proteins with a Y-shaped amino acid chain structure produced in the plasma cells. Their role in the immune system is essential. They identify and target pathogens, including viruses and bacteria. Their high affinity, small size, and fast genetic manipulation make them robust and valuable units for immunosensors devising. There are polyclonal and monoclonal

antibodies; both are widely used in medical research [26], diagnostics [27], and immunosensing [28]. Typically, polyclonal antibody production is based on the injection of a lab animal with specific antigens, and then, after the immunological response of the animal, the produced specific antibodies are collected as an antiserum [29]. In contrast, monoclonal antibodies are produced in vitro. The production starts with immunizing a lab animal, generally a mouse, and then the desired antibodies are selected and grown using the tissue culture technique. The culture medium is periodically collected, followed by the purification of monoclonal antibodies from the medium [30].

EC immunosensors using antibodies as recognition units have revolutionized diagnostics because of cancer biomarkers determination. One of the most crucial steps in devising these immunosensors is the antibodies' tethering to solid support without affecting their biological activity and specificity, then translating to the overall immunosensor performance from sensitivity to the limit of detection (LOD). Three strategies for antibody immobilization have so far been proposed. The simplest one is the non-covalent immobilization, mainly based on antibodies' adsorption onto the electrode surface [31]; it could be either chemisorption or physisorption, including van der Walls forces and hydrophobic or electrostatic interactions. Covalent immobilization has been extensively studied in EC immunosensors for cancer biomarkers. The principle of this strategy is to modify the electrode surface with reactive groups, including carboxyl, thiol, or hydroxyl groups, to bind antibodies covalently. THis modification is helpful in immunosensor storage and reusability [32]. Despite the advantages of covalent immobilization, it still has some drawbacks, such as the false orientation of antibodies. Affinity-based immobilization can overcome that to produce correctly oriented active antibodies attached to the sensing platform [33]. Two main modes have been developed for the EC immunosensing of cancer biomarkers, i.e., label-free and sandwich-type modes (Fig. 1).

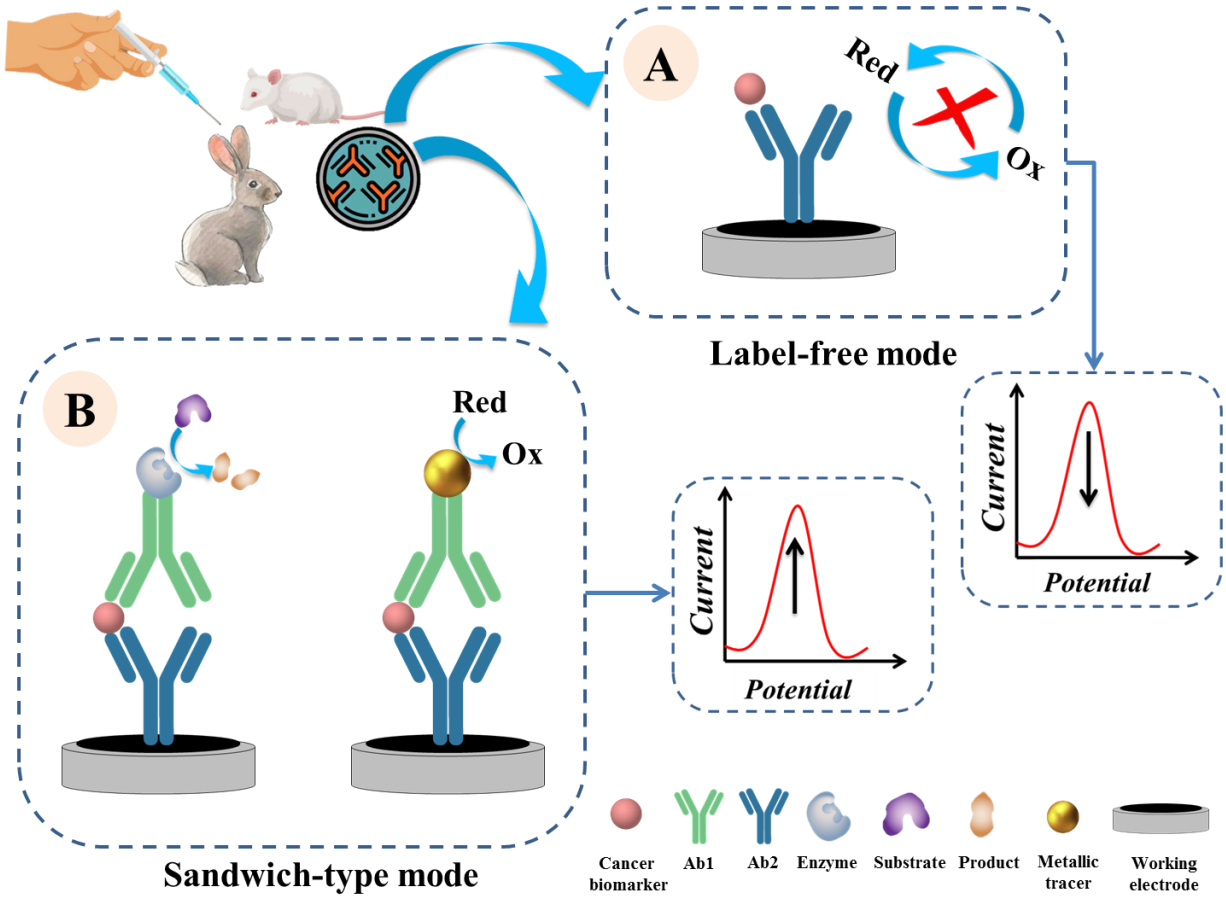

Fig. 1. Schematic illustration of preparation, structure, and operation of electrochemical cancer biomarker sensors with recognition units of (A) label-free and (B) sandwich-type antibodies.

Principle of the EC label-free antibody-based detection of cancer biomarkers

Generally, devising an EC label-free immunosensor for a cancer biomarker based on antibodies involves two main steps. The first is the modification of the working electrode surface with nanomaterials such as the carbon, carbon derivate, and metal nanoparticles (NPs), as well as the activation of the sensing support with carboxyl or amine groups to improve the EC sensing properties, increase the electrode active surface area and enhance the loading capacity of antibodies. The second step is to immobilize the chosen antibodies, which are naturally specific toward a targeted cancer biomarker, using one of the three strategies, i.e., non-covalent, covalent, and affinity immobilization. The biomarker detection and determination are based on the ion channel mimetic principle, necessitating the presence of a redox probe because cancer biomarkers are electrochemically inactive. This probe accessibility towards the electrode surface is suppressed

after interacting antibody with the cancer antigen, forming the antibody-antigen complex (Fig. 1). This signal generation by ion-channel mimetics can be followed with EC techniques, including cyclic voltammetry (CV), differential pulse voltammetry (DPV), square wave voltammetry (SWV), and electrochemical impedance spectroscopy (EIS) [34]. The most used redox probe in cancer biomarker sensing is the $Fe(CN)_6^{3-}/Fe(CN)_6^{4-}$ redox couple for its high EC activity and reversibility.

Electrochemical label-free cancer biomarker immunosensors

In the realm of cancer biomarker detection, researchers have harnessed diverse strategies to enhance the sensitivity and accuracy of their assays. In the case of CEA detection, an immunosensor has been devised based on a label-free approach using natural antibodies as the recognition unit. Li et al. [35] employed reduced graphene oxide (rGO), PtNPs, and AuNPs to enhance the active surface area for antibody immobilization. The CEA analyte was determined using SWV in the presence of the H_2O_2 redox probe. The interaction of antibodies with antigens on the matrix active surface and non-electroactive substrate (protein) blocking the electrode surface and slowing down the diffusion of H_2O_2 was the reason for the current signal decrease with the CEA concentration increase. The sensor was highly sensitive at very low CEA concentrations, displaying a LOD of 7 fg mL^{-1} and a linear dynamic concentration range of 10 to 10^8 fg mL^{-1}. The sensor excellently discriminated between the target biomarker and potential interferents, including ascorbic acid, BSA, L-tryptophan, and α-fetoprotein.

Moreover, conductive polymers, e.g., polyaniline (PANI), have extensively been used in devising EC immunosensors for cancer biomarkers for their featured characteristics, from biocompatibility to high surface area, high electrical conductivity, and antifouling capability. Besides, the PANI redox transition between the emeraldine and leucoemeraldine, manifested in EC analysis curves, can be employed as a reference for quantifying a non-electroactive substrate. PANI and the poly(carboxybetaine methacrylate) (polyCBMA) composite were used for preparing a label-free sensor for CEA [36]. The proposed anti-CEA/polyCBMA/PANI/GCE matrix was a stable, biocompatible platform for antibody immobilization, especially using polyCBMA to block non-specific adsorption sites. DPV peaks were inversely proportional to the logarithm of the CEA concentration between 1.0×10^{-14} and 1.0×10^{-10} g mL^{-1} with a LOD of 3.02 fg ml^{-1}. Moreover, a

high selectivity was demonstrated for the target biomarker against prostate-specific antigen (PSA) and α-fetoprotein (AFP)-similar biomarkers.

Gold nanomaterials are very popular in electrode modification, especially when immobilizing important bio-compounds, such as antibodies. Besides their biocompatibility, they are electric conductors of high conductivity [37]. Cai et al. [38] fabricated an EC immunosensor for CEA based on polythionine-(gold nanoparticles) (PTh-AuNPs) as the matrix to immobilize CEA antibodies and enhance the EC signal. DPV was used for CEA determination, and the $Fe(CN)_6^{3-}$/$Fe(CN)_6^{4-}$ probe appeared helpful as the signal indicator for protein detection and quantification. The immunosensor's LOD and linear dynamic concentration range were 2.2 pg mL^{-1} and 0.005 to 40 ng mL^{-1}, respectively. Butmee et al. [39] devised another label-free EC immunosensor for CEA. They anchored CEA antibodies to core-shell Fe_3O_4@AuNPs. That was to exploit the magnetic properties of Fe_3O_4 using an external magnet for capturing CEA to the surface of the screen-printed carbon electrode (C-SPE). Before the CEA determination, C-SPE was modified with graphene nanoplatelets and the MnO_2 nanomaterial to enhance the electron transfer further and enlarge the electrode's active surface area. Core-shell magnetic Fe_3O_4@AuNPs appeared useful for antibody immobilization and signal amplification. The devised sensor determined CEA using the linear sweep voltammetry (LSV) in the linear dynamic concentration range of 0.001 to 100 ng mL^{-1} with a LOD of 0.10 pg mL^{-1}. Its precision in detecting CEA was remarkable, minimizing false positives when tested against ten interfering agents, including proteins and small-molecule biocompounds, including glucose, sucrose, cysteine, ascorbic acid, and uric acid. Another study expanded the use of a samarium rare-earth metal in developing new metal-organic frameworks (MOFs) for EC immunosensing of CEA. The fabricated rare-earth metal MOFs served as efficient platforms for CEA-specific antibody immobilization [40].

Most π-electron conjugated polymers are highly conductive, revealing exceptional optical features and energy consumption. Therefore, they are referred to as "synthetic metals." Amine and carboxyl functional groups, which can be present in these polymers, may be used for anchoring biomolecules. Shifting this idea to Cancer antigen 125 (CA 125) sensing, it was performed using the poly(3-hydroxyphenyl acetic acid) support in a label-free EC mode. A $Fe(CN)_6^{3-}$/$Fe(CN)_6^{4-}$ probe was used to determine the actual CA 125 concentration. The sensor reached a 1.45 U mL^{-1} LOD and a linear dynamic concentration range of 5 to 80 U mL^{-1} based on DPV response.

However, solely relying on serum samples in this study does not provide a complete assessment of selectivity; direct interfering agents are essential [41].

In today's advanced technology and smart devices era, new intelligent devices are fabricated for self-use and testing, as described, e.g., in [42]. This study reports on an electrochemical immunosensor for CA 125 determination based on a smartphone. The device comprised an electrochemical system with SPEs and a smartphone to display the DPV results. The immunosensor determined CA 125 with a LOD of 2 mU mL^{-1} in a linear dynamic concentration range between 1.3 and 260 U mL^{-1}.

For Cancer antigen 19-9 (CA 19-9) detection, Huang et al. [43] electrochemically determined CA 19-9 using label-free PTh-AuNPs composites for signal amplification. They prepared an EC sensor by GCE coating with AuNPs as the first layer. Then, they modified this layer with PTh-AuNPs composites followed by immobilization of antibodies (Fig. 2). The CV curves demonstrated effective signal amplification. The DPV linear dynamic concentration range was 6.5 to 520 U mL^{-1} using the $Fe(CN)_6^{3-}/Fe(CN)_6^{4-}$ probe as the signal indicator; a LOD achieved was 0.26 U mL^{-1}. Moreover, this immunosensor cross-reactivity with other substances that might be present in the sample, like CEA, AFP, and CA 125, was minimal.

For differentiation-44 cluster (CD44) antigen quantification in clinical samples, a DPV and EIS dual-mode determination was proposed. The sensing platform was structured by immobilizing antibodies on the hybrid nanomaterial surface of GO, ionic liquid, and gold nanoparticles. The immunosensor for CD44 exhibited a linear detection range spanning from 5.0 fg mL^{-1} to 50.0 µg mL^{-1}. Notably, the LOD was 2.0 fg mL^{-1} and 1.90 fg mL^{-1} when assessed through DPV and EIS, respectively. In this study, the EIS's ability to outperform DPV in terms of precision is particularly intriguing, substantiated by the attainment of a lower LOD. This assertion underscores the power of EIS to delve deeper into the electrochemical nuances at the interface, possibly yielding more distinct insights into the molecular interactions and events underpinning the quantification [44].

Lastly, in the pursuit of simultaneous determination of multiplexed cancer biomarkers, which seems complicated in the label-free mode, but that did not stop researchers from attempting; only one report was found in this regard where a multi-array electrode system was proposed for simultaneous CV determination of CEA, CA 125, Cancer antigen 15-3 (CA 15-3), and CA 19-9

[45]. The idea was to modify each working electrode array with an antibody specific to a given biomarker. However, generating a simultaneous signal for each biomarker is impossible in real applications. Each modified array is tested individually, so the term "simultaneous" is not applicable here. That is one of the most significant inconveniences of label-free EC immunosensing.

Table 2. Electrochemical label-free antibody-based sensors for cancer biomarkers.

Electrode modification	**Target biomarker**	**Signal tranduction technique**	**Linear dynamic concentration range**	**Limit of detection**	**Number of interfering agents**	**Storage stability (days)**	**Ref.**
GCE/rGO-PtAu1/BSA/Ab	CEA	SWV	10 to 10^8 fg mL^{-1}	7 fg·mL^{-1}	4	20	[35]
GCE/polyCBMA/PANI/Ab	CEA	DPV	0.1 pg mL^{-1} to 10 ng mL^{-1}	3.05 fg mL^{-1}	4	-	[36]
GCE/AuNPs/PTh-Au/BSA/Ab	CEA	DPV	0.005 to 40 ng mL^{-1}	2.2 pg mL^{-1}	5	-	[38]
C-SPE/GNPMnO2/Fe_3O_4@Au-Ab	CEA	LSV/EIS	0.001 to 100 ng mL^{-1}	0.10 pg mL^{-1}	10	7	[39]
C-SPE/poly(3-HPA)/Ab	CA 125	DPV	5 to 80 U mL^{-1}	1.45 U mL^{-1}	-	20	[41]
C-SPE/MWCNTs/Thi/AuNPs	CA 125	DPV	1.3 to 260 U mL^{-1}	2 U mL^{-1}	-	-	[42]
GCE/AuNPs@PThi/BSA/Ab	CA 19-9	DPV	6.5 to 520 U mL^{-1}	0.26 U mL^{-1}	7	-	[43]
GCE/GO-IL-AuNPs/Ab	CD44	DPV EIS	5.0 fg mL^{-1} to 50.0 µg mL^{-1}	2 fg mL^{-1} 1.9 fg mL^{-1}	-	-	[44]
GCE/ZrO_2-rGO-IL/BSA/Ab	CEA	DPV	25.0 fg mL^{-1} to 25.0 ng mL^{-1}	16 fg mL^{-1}	-	-	[46]
ITO/MWCNTs/PDDA/HA/BSA	CD44	DPV	0.01 to 100 ng mL^{-1}	5.94 pg mL^{-1}	-	14	[47]
VA-MWCNT electrode/ssDNA	CEACAM5	CV	50 to 250 µM	0.92 µM	-	7	[48]
GCE/PEDOT/PEP/DNA(C1)/MB	BRCA1	DPV	0.01 pM to 1 nM	0.0034 pM	4	-	[49]
GCE/3D-rGO-PANI/ssDNA	BRCA1	DPV	1 fM to 0.1 µM	0.301 fM	3	30	[50]
AuE/rGO-COOH/PdAuPt/EDC/NHS Ab	CEA	DPV	12 pg mL^{-1} to 85 ng mL^{-1}	8 pg mL^{-1}	6	40	[51]
AuE/rGO-COOH/PdAuPt/EDC/NHS Ab	PSA		3 pg mL^{-1} to 60 ng mL^{-1}	2 pg mL^{-1}		-	
C-SPE1/2,3-diaminophenazine-AuNPs/Ab	CA 15-3	DPV	-	0.14 U mL^{-1}	-	-	[52]
C-SPE2/TB-AuNPs/Ab	RNA-21		-	1.2 fM			

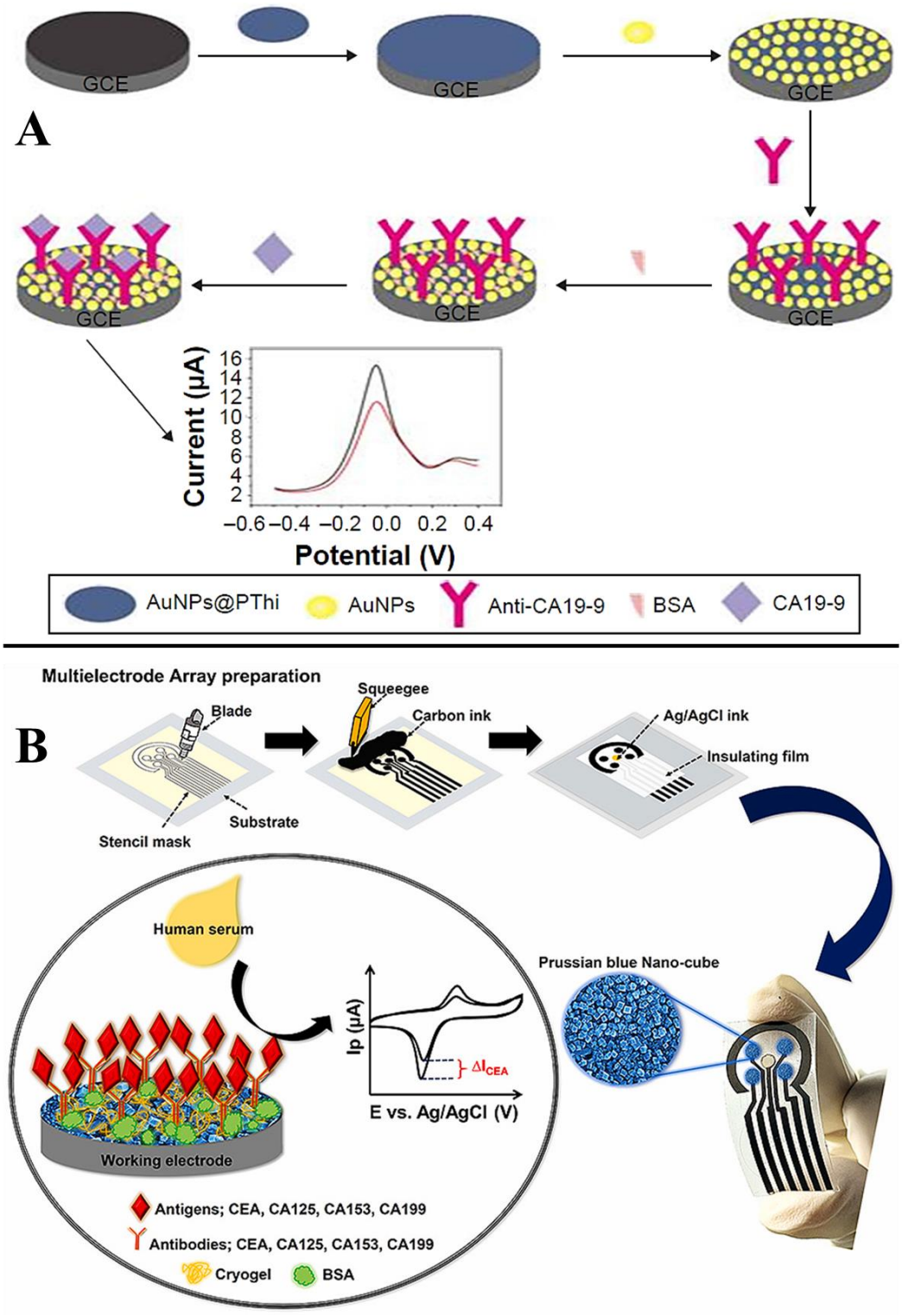

Fig. 2. (A) The label-free electrochemical immunoassay preparation and operation flow chart for carbohydrate antigen 19-9 based on polythionine-AuNPs composites. (Reproduced with permission from

Ref. [43]**)**, and (B) Preparation of multi-array electrode for simultaneous determination of CEA, CA 125, CA 15-3, and CA 19-9. (Reproduced with permission from Ref. [45]).

Principle of the EC sandwich-type antibody-based detection of cancer biomarkers

Typically, in the label-free EC immunosensor, the generated signal decreases with the increase of the biomarker concentration, meaning that the highest signal will appear at zero concentration. The variation in the signal height cannot sometimes be detected at low concentrations used to simulate the concentrations in human body fluids. In contrast, the sandwich-type EC immunosensor, which illustrates the noncompetitive immunoassay format, offers the highest selectivity and sensitivity due to using two matched antibodies sandwiching the target biomarker (Fig. 1) [53]. This approach aims to measure the labeled analyte (generally secondary antibodies) concentration, proportional to the concentration of the cancer antigen present in the sample tested. For signal amplification, labels are employed by combining secondary antibodies with enzymes to generate an enzymatic amplification that necessitates another redox probe in the sample. Alternately, these labels can be combined with a metal tracer, thus generating an EC signal through a redox reaction. Moreover, using nanostructures as nanocarriers for secondary antibodies and enzymes or metal nanotracers can further enhance the labels' loading capacity, resulting in an enhanced EC signal [54]. This detection and quantification concept principle is that increasing antigen concentration enables more labels to be attached to the electrode surface via secondary antibodies, thus increasing the analytical signal generated [55].

Electrochemical sandwich-type immunosensors for cancer biomarkers

Hybridization of nanomaterials, including graphene and noble metals, is very efficient in EC immunosensing because of elevating the conductivity and enlarging the active electrode area, two factors essential for improving immunosensor performance [56]. Furthermore, noble metals are highly biocompatible, thus being perfect candidates for antibodies' and enzymes' immobilization. Illustrating this with a case in cancer embryonic antigen (CEA) determination, Nakhjavani et al. [57] devised an EC sandwich-type immunosensor using thiolated graphene oxide (T-GO) and streptavidin-AuNPs nanocomposites to immobilize primary antibodies on the GCE surface. Moreover, the enzymatic amplification probe, streptavidin-AgNPs nanocomposite, was used to carry the secondary antibodies and horseradish peroxidase (HRP). With DPV in the presence of

H_2O_2 as the redox probe, the immunosensor reached a very low LOD of 75 fg mL^{-1}, and a linear dynamic concentration range extended from 100 fg mL^{-1} to 5 pg mL^{-1}. This immunosensor's exclusivity ensures that it primarily responds to CEA in the presence of PSA, BSA, p53, and AFP.

Considering another aspect, the immunosensor loading capacity is a crucial factor that makes a highly porous structure advantageous to generating more active sites for antibody immobilization. That results in enhancing antibody-antigen interactions. On this basis, Ma et al. [58] prepared CoS_2@C 3D hollow sheet nanotubes as the carrier for CEA secondary antibodies and HRP. AuNPs were used as the solid support for primary antibody immobilization. The CEA immunosensor was highly electrocatalytic and active toward H_2O_2 decomposition, demonstrated by its high amperometric response in the linear dynamic concentration range of 0.001 to 80 ng mL^{-1} with a LOD of 0.33 pg mL^{-1}. Minimal cross-reactivity with other substances might be present in the sample when testing with AFP, BSA, HRP, dopamine, and ascorbic acid. In the same context, MoS_2-containing nanomaterials have remarkable potential for electrode modification due to their high active surface area, enhancing the loading capacity by providing more active sites for antibodies. Su et al. [59] explored these nanomaterials' performance as a platform for primary antibodies. As a signal amplification probe, MoS_2 nanosheets were coupled with AuNPs and HRP for multiple signal amplification. DPV linear dynamic concentration range stretched from 10 fg mL^{-1} to 1 ng mL^{-1} CEA, and a LOD was ultra-low, attaining 1.2 fg mL^{-1}. AFP, BSA, and IgG were selected as interfering species, and the selectivity test demonstrated low interference from these non-specific molecules.

Solving the problems of enzyme deactivation by mimicking enzymes' catalytic activity based on noble metals and nanocomposites could decrease the costs and improve the stability and efficiency of immunosensors. Tan et al. [60] devised an amperometric immunosensor for CEA of selective affinity even in the presence of AFP, BSA, and IgG. They reached a high peroxidase activity by employing graphene-supported PdNPs and AuNPs for secondary antibodies. Peroxidase activity of this immunosensor was intense, and the amperometric linear dynamic concentration range was 10 fg·mL^{-1} to 100 ng·mL^{-1} with a LOD of 3.2 fg·mL^{-1}. Similarly, Zhao et al. [61] studied the AgNPs' catalytic activity toward H_2O_2 electroreduction and its application for CEA immunosensor devising. An (AgNPs-PANI)/MnO_2 hybrid nanocomposite was synthesized and used as the amplification probe (Fig. 3). The DPV linear dynamic concentration range and LOD were 0.0005

to 80 ng mL^{-1} and 0.17 pg mL^{-1}, respectively. This immunosensor's high discriminatory capability ensures it responds only to CEA, and the presence of interferants, including AFP, HRP, BSA, dopamine, and ascorbic acid, displayed less than 5% perturbation, confirming the excellent selectivity. Ma et al. [62] devised another immunosensor for CEA. That was based on mimicking peroxidase activity. The authors conjugated secondary antibodies on a hybrid nanocomposite constructed from gold, silver, and platinum, combined in a cubic shape, and loaded on amino-functionalized MoS_2 nanoflowers. Triangle AuNPs were synthesized to attach primary antibodies to the carbon electrode surface. The active surface area of the as-synthesized nanomaterials was enlarged effectively, and catalytic activity toward H_2O_2 electroreduction was intense, enhancing the current signal. The amperometric linear dynamic concentration range was 10 fg mL^{-1} to 100 ng mL^{-1} with a LOD of 3.09 fg mL^{-1}. The CEA immunosensor is well-guarded against producing false alarms due to non-specific interactions, validated in the presence of PSA, hepatitis B, BSA, and AFP.

Elaborating further on CEA determination, integrating an electroactive metal nanotracer in the amplification label eliminates the need to use enzymes [63]. (Molybdenum disulfide)-(cerium oxide) (CeO_2-MoS_2) nanocomposite was the carrier of Pb^{2+} and a secondary antibody, with AuNPs applied for primary antibody immobilization. The SWV signal of Pb^{2+} linearly depended on the CEA concentration in the range of 0.001 to 80 ng mL^{-1} with a LOD of 0.3 pg mL^{-1}, and cross-interfering with other analytes such as AFP, BSA, dopamine, and HRP was negligible, ensuring accurate readings.

Moreover, ferrocene (Fc) and its derivatives are widely used as the EC signal probe. Integrating Fc with the signal amplification probe in a sandwich-type immunoassay effectively eliminated the use of enzymes. Incorporating Fc with polymers and nanomaterials is necessary to increase stability to prevent Fc leakage. Chen et al. [64] used this electroactive probe for CEA determination. They synthesized hybrid metal nanocrystals, {PdAuCu}, and then combined them with Fc-grafted-polylysine (Fc-g-PLL) for loading secondary antibodies and AuNPs as a platform for primary antibodies. The immunosensor linear dynamic concentration range was broad, extending from 0.001 to 100.0 ng mL^{-1}, and the LOD was 0.23 pg mL^{-1}. The sensor was validated for CEA determination in human serum, providing an almost exclusive response to CEA, in contrast to the interfering agents (PSA, AFP, BSA, and CA 125).

Moreover, thiolated Fc (Fc-SH) with AuNPs was directly incorporated into the construct of a CEA sensor. The formation of covalent bonds between sulfur and gold atoms can facilitate the Fc–SH immobilization on the surface of AuNPs to result in a highly stable film. The sandwich-type sensor displayed an SWV linear dynamic concentration range of 0.05 to 20 ng mL^{-1} CEA with an LOD of 0.01 ng mL^{-1}. Moreover, the selectivity was deeply investigated using an excessive concentration of glucose, cysteine, BSA, IgG, and PSA, revealing a shallow signal perturbation [65].

Graphene-metal nanomaterials can be introduced in a sandwich-type immunoassay for bio-compounds determination due to their high conductivity and large active surface area. Accordingly, using highly biocompatible noble metals for antibodies and enzyme immobilization, Chen et al. [66] invented an amperometric immunosensor for CEA. The conductivity and loading capacity of antibodies and HRP were remarkably improved by using an AuNPs-TiO_2-GR nanocomposite as the amplification probe. The amperometric linear dynamic concentration range was 0.005 to 200 ng mL^{-1} CEA, and the LOD was 3.33 pg mL^{-1}; however, the selectivity was in question when testing with AFP, thrombin, IgG, and osteopontin, reaching 17% in signal perturbation.

Loading different metal ions on the amplification probe as an electroactive nano-tracer enhances the electron transfer accompanying the EC reaction. As a result, current responses are higher, and LODs are lower. This strategy was demonstrated by Pothipor et al. [67] in the realm of PSA determining, where they loaded copper ions onto Ag-Au hybrid NPs with a hollow porous structure. That was to enlarge the surface area for anchoring copper ions and secondary antibodies, thus increasing the conductivity. The electrode surface was modified with GR-(conductive polymer) composite as the solid support for primary antibodies. The resulting EC immunosensor was highly selective against CEA, IgG, and BSA PSA, detecting PSA up to 80 ng mL^{-1} with a LOD of 0.13 pg mL^{-1}.

In the same context for PSA sensing, Ehzaris et al. reported [68] an enzyme-free EC immunosensor for PSA investigating Ni-Cd quantum dots' performance as secondary antibodies' labels. With their high conductivity, those dots revealed a DPV current signal at -0.83 V related to the presence of cadmium. This signal was further employed to construct the calibration curves for PSA. The authors used magnetic FeNPs with MOFs for electrode modification to enhance the conductivity and enlarge the active surface area. These results demonstrated the effective use of quantum dots

as labels and, simultaneously, as electroactive probes. Advantageously, the LOD of this PSA immunosensor was low, equaling 0.45 pg mL^{-1}, and a DPV linear dynamic concentration range was 1 pg mL^{-1} to 100 ng mL^{-1} with solid resistance to interference from substances commonly found in complex biological matrices, as validated for BSA, hepatitis B, CEA, and IgG.

Moving on to AFP determination, a major plasma protein, Wang et al. [69] developed a sensitive pseudo-ELISA test. For that, the secondary and primary antibodies were immunologically reacted with AFP in a microplate, and then the sandwich-type immunological complex was drop-cast on the surface of a screen-printed electrode (SPE) modified with AgNPs (Ag-SPE). Tubular Co_3O_4@MnO_2-thionine nanomaterials were used as carriers for secondary antibodies to increase the active surface area and enhance the current response. The DPV linear dynamic concentration range was wide, covering 0.001 to 100 ng mL^{-1}, and a LOD was 0.33 pg mL^{-1}. However, a label-free comparative study is necessary to evaluate the performance of a sandwich-type EC immunosensor [70]. In this context and based on a similar amplification strategy, two AFP immunosensors were proposed by modifying a GCE surface with Au-Pt and vertical graphene (VG) nanocomposites. The difference was the addition of the secondary antibody labels in the sandwich-type mode. The labels were prepared using carbon nanotubes (CNTs), AuNPs, and methyl orange (MO) as the electroactive probes. Both immunosensors demonstrated an outstanding performance toward AFP determination from 1 fg mL^{-1} to 100 ng mL^{-1}. However, in terms of LOD and sensitivity, the sandwich-type sensor showed higher results {43.3 μA [log(pg mL^{-1})]$^{-1}$} and 0.7 fg mL^{-1}, respectively. The selectivity tests showed less than 7% of signal perturbation in the presence of CEA, CA 125, CA 19-9, and CA 15-3, considered acceptable.

Moreover, CA 125 was determined using an EC immunosensor prevailingly containing rGO as the highly porous conductive nanomaterial based on the sandwich mode. Wang et al. [71] employed rGO and thionine chloride to devise the amplification probe. Thionine chloride (Thic) was used to attach the secondary antibodies. Primary antibodies were adsorbed on rGO after immunologically reacting antibodies in the presence of CA 125. Thus, the rGO/Thic/Ab2/CA 125/ab1/rGO sandwich was constructed and transferred onto the GCE surface preliminary modified with AuNPs and BSA. The DPV response revealed the sensor's high catalytic activity toward O_2 electro-reduction to H_2O, which was useful for constructing the calibration curve. The lowest and the highest values detected were 4.10 and 2 μg mL^{-1}, respectively. Real human serum samples were

also tested. However, selective discrimination should extend beyond serum constituents, requiring direct interfering agents.

Electrochemical sandwich-type antibody-based sensors for simultaneous multiplexed determination of cancer biomarkers

One of the most explored strategies for the simultaneous EC determination of multiplexed biomarkers involves electroactive metal ions as selective tracers. This strategy involves modifying a conductive platform, generally an electrode, with antibodies specific to the target biomarkers. After antibodies react with different biomarkers on the electrode surface, the secondary antibodies, labeled with metal ions, are introduced onto this modified surface to complete the sandwich-type immunological reaction. Then, each metal ion quantity is related to a given biomarker concentration, corresponding to an EC signal. Following this strategy, Kalyoncu et al. [72] simultaneously determined AFP, vascular endothelial growth factor (VEGF), and CEA. They modified C-SPE with anti-AFP, anti-VEGF, anti-CEA, and then BSA to block non-specific recognizing sites. Au-magnetic nanoparticle hybrid labels were loaded with Zn, Cu, and Pb to trace AFP, VEGF, and CEA, respectively (Fig. 4). DPV peaks of the metal ions recorded corresponded to biomarkers' concentrations.

Similarly, Yu et al. [73] reported on a ratiometric immunosensor for multiplex cancer biomarkers. They used metal sulfide as the secondary antibody label to measure distinguishable current signals simultaneously. Cd(II), Hg(II), Pb(II), and Zn(II) were used as tags for AFP, CA 19-9, CA 125, and CEA, respectively. Using a bismuth film as an internal reference was investigated, demonstrating the ability to improve the anodic stripping voltammetry results with well-separated peaks. AFP, CA 19-9, CA 125, and CEA were successfully determined, with respective LODs of 0.11 pg mL^{-1}, 0.68 mU mL^{-1}, 1.4 mU mL^{-1}, and 0.23 pg mL^{-1}. Although the serum samples were tested, they were diluted 50 times, minimizing the possibility of cross-interfering; thus, incorporating direct interfering agents into the selectivity testing process can provide a more comprehensive evaluation of the sensor's performance and its ability to differentiate the target cancer biomarker from potential interferents in real-world scenarios.

The simultaneous determination of protein biomarkers can generally be successful if current signals are generated separately to identify and quantify each biomarker. Further, using different

electroactive substrates as nanoprobe tags improves sensitivity and selectivity. For instance, Wang et al. [74] used anthraquinone (Aq) and Fc as tracers for CEA and AFP integrated with PDA-MWCNTs and secondary antibodies. In contrast, primary antibodies were attached to the surface of GCE, and non-specific recognizing sites were blocked with BSA. With the DPV transduction, the sensor was highly sensitive to CEA and AFP, reaching 56.1 fg mL^{-1} and 32.8 fg mL^{-1} LODs, and the linear dynamic concentration ranges of 163 fg mL^{-1} to 163 ng mL^{-1} and 100 fg mL^{-1} to 100 ng mL^{-1}, respectively. The sensor was selective to CEA and AFP, demonstrating low interference from PSA, BSA, glutaraldehyde, and ascorbic acid.

Moreover, researchers are racing to develop new procedures enabling the simultaneous EC determination of protein biomarkers by generating separable current signals for the biomarkers studied. For example, Li et al. [75] developed a new creative strategy to determine CEA and AFP accurately based on the current signal difference in a chronoamperometric response. For that, mesoporous $PdAgCeO_2$ nanobeads and MnO_2 nanosheets were used as the non-enzymatic catalysts for H_2O_2 electroreducing, as well as labeling CEA and AFP secondary antibodies, respectively. After the immune reaction (sandwich-type mode), the sensor was tested using chronoamperometry, followed by the elimination of MnO_2 nanosheets with ascorbic acid, and then tested again. Expectedly, the current changed because of the decreased electrode catalytic activity. This electrical signal difference can indicate the amount of the MnO_2 nanosheets present. That can correspond to the amount of AFP based on the sandwich-type EC sensor operation. CEA was quantified using the current signal generated after MnO_2 nanosheets were entirely eliminated. The sensor accurately determined CEA and AFP, achieving low LODs of 0.5 and 1 pg mL^{-1}, respectively, and broad respective linear dynamic concentration ranges of 0.001 ng mL^{-1} to 40 ng mL^{-1} and 0.005 ng mL^{-1} to 100 ng mL^{-1}. Dopamine, ascorbic acid, PSA, and CA 125 were employed for the selectivity study, and the immunosensor demonstrated its ability to distinguish CEA and AFP from interfering compounds.

Table 3. Electrochemical sandwich-type antibody-based sensors for cancer biomarkers determination in serum samples.

Immunological platform	Signal amplification probe	Target biomarker	Signal tranduction technique	Limit of detection	Linear dynamic concentration range	Number of interfering agents	Storage stability (days)	Ref.
GCE/T-GO/Strp-AuNPs/Ab1	Strp-AgNPs-HRP/Ab2	CEA	DPV	75 fg mL^{-1}	0 to 5pg mL^{-1}	3	15	[57]
GCE/AuNPs/Ab1/BSA	CoS_2@$CeNH_2$-HRP-Ab2	CEA	Amperometry	0.33 pg mL^{-1}	0.001 to 80 ng mL^{-1}	5	30	[58]
GCE/AuNPs/MoS_2/Ab1/BSA	HRP/HRP-Ab2/MoS_2-AuNPs	CEA	DPV	1.2 fg mL^{-1}	10 fg mL^{-1} to 1 ng mL^{-1}	3	16	[59]
GCE/NPs/CE-Au/Ab1/BSA	GO supported G-Au/Pd-Ab2	CEA	Amperometry	3.2 fg mL^{-1}	10 fg mL^{-1} to 100 ng mL^{-1}	3	30	[60]
GCE/AuNPs/Ab1/BSA/	Ab2-Ag-PANI@MnO_2	CEA	DPV	0.17 pg mL^{-1}	0.0005 to 80 ng mL^{-1}	5	30	[61]
GCE/AuTNPs/Ab_1/BSA	MoS_2-NFs/Au@AgPtYNCsAb2	CEA	Amperometry	3.09 fg m L^{-1}	10 fg mL^{-1} to 100 ng mL^{-1}	4	25	[62]
GCE/Au/Ab1/BSA	CeO_2/MoS_2/Pb^{2+}/BSA/Ab2	CEA	SWV	0.3 pg mL^{-1}	0.001 to 80 ng mL^{-1}	4	20	[63]
GCE/AuNPs/BSA/Ab1	Fc-g-PLL/PdAuCu NCs/Ab2	CEA	DPV	0.23 pg mL^{-1}	0.001 to 100.0 ng mL^{-1}	4	12	[64]
AuE/LPA-NHS/Ab1	Ab2-AuNPs-Fc	CEA	SWV	0.01 ng mL^{-1}	0.05 to 20 ng mL^{-1}	5	21	[65]
GCE/AuNPs/BSA/Ab1	HRP-Ab2-AuNPs-TiO_2-GR	CEA	DPV	3.33 pg mL^{-1}	0.005 to 200 ng mL^{-1}	4	15	[66]
GP modified C-SPE/EDC/NHS/AntiPSA	Cu^{2+}-PHSGNP-Ab2	PSA	DPV	0.13 pg mL^{-1}	-	3	30	[67]
GCE/MOF-CS/BSA/Ab1	Ab2-QDs	PSA	DPV	0.45 pg mL^{-1}	1 pg mL^{-1} to 100 ng mL^{-1}	4	14	[68]
C-SPE/AgNPs/Ab1	Ab2-Co_3O_4@MnO_2-Th	AFP	DPV	0.33 pg mL^{-1}	0.001 to 100 ng mL^{-1}	4	20	[69]
GCE/AuPt-VG-Ab1	MO/CNT-Au/Ab2	AFP	DPV	0.7 fg mL^{-1}	1 fg mL^{-1} to 100 ng mL^{-1}	4	30	[70]
rGO/AuNPs/BSA/X306/Ab1	rGO/AuNPs/BSA/X306/Ab2	CA 125	DPV	4.10 pg mL^{-1}	-	-	-	[71]
SPE/GA/Ab1-CEA, Ab1-VEGF, Ab1-AFP	Ab2-CEA-PbAu@ɣFe_2O_3 Ab2-VEGF-CuAu@ɣFe_2O_3 Ab2-AFP-ZnAu@ɣFe_2O_3	CEA AFP VEGF	DPV	-	-	-	-	[72]
GCE / MSA-CNT-ATA /Ab1-(AFP, CEA, CA 19-9, CA 125)	CdS-Ab2-AFP	AFP	DPASV	0.11 pg mL^{-1}	1 pg mL^{-1} to 10 ng mL^{-1}	-	-	[73]
	ZnS-Ab2-CEA	CEA		0.23 pg mL^{-1}	1 pg mL^{-1} to 10 ng mL^{-1}			
	HgS-Ab2-CA 19-9	CA 19-9		0.68 mU mL^{-1}	0.004 to 100 U mL^{-1}			
	PbS-Ab2-CA 125	CA 125		1.4 mU mL^{-1}	0.004-100 U mL^{-1}			
GCE/PdAg/Ab1-(AFP, CEA)/BSA	PdAgCeO_2-Ab2-CEA	CEA	Amperometry	0.5 pg mL^{-1}	0.001 ng mL^{-1} to 40 ng mL^{-1}	4	20	[74]
	MnO_2-COOH-Ab2-AFP	AFP		1pg mL^{-1}	0.005 ng mL^{-1} to 100 ng mL^{-1}			
GCE /AuNPs/Ab1(AFP, CEA)/rGO/	Fc/PGMA-g-MWCNTs/Ab2-AFP	AFP	DPV	32.8 fg mL^{-1}	100 fg mL^{-1} to 100 ng mL^{-1}	5	-	[75]
	Aq/PGMA-g-MWCNTs/Ab2-CEA	CEA		56.1 fg mL^{-1}	163 fg mL^{-1} to 163 ng mL^{-1}			

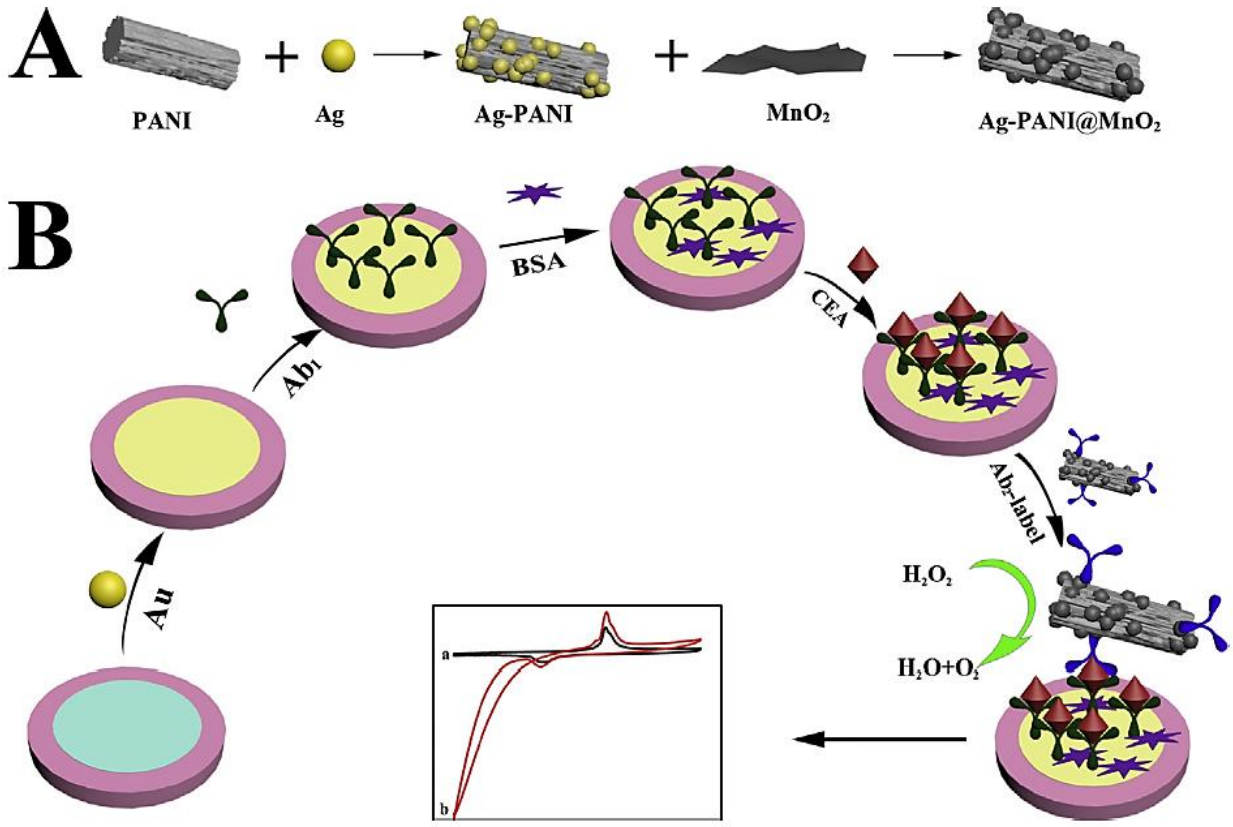

Fig. 3. The flowchart for EC immunosensing of CEA with a sandwich-type immunosensor. (A) The label preparation, and (B) the immunosensor fabrication steps. (Reproduced with permission from Ref. [61]).

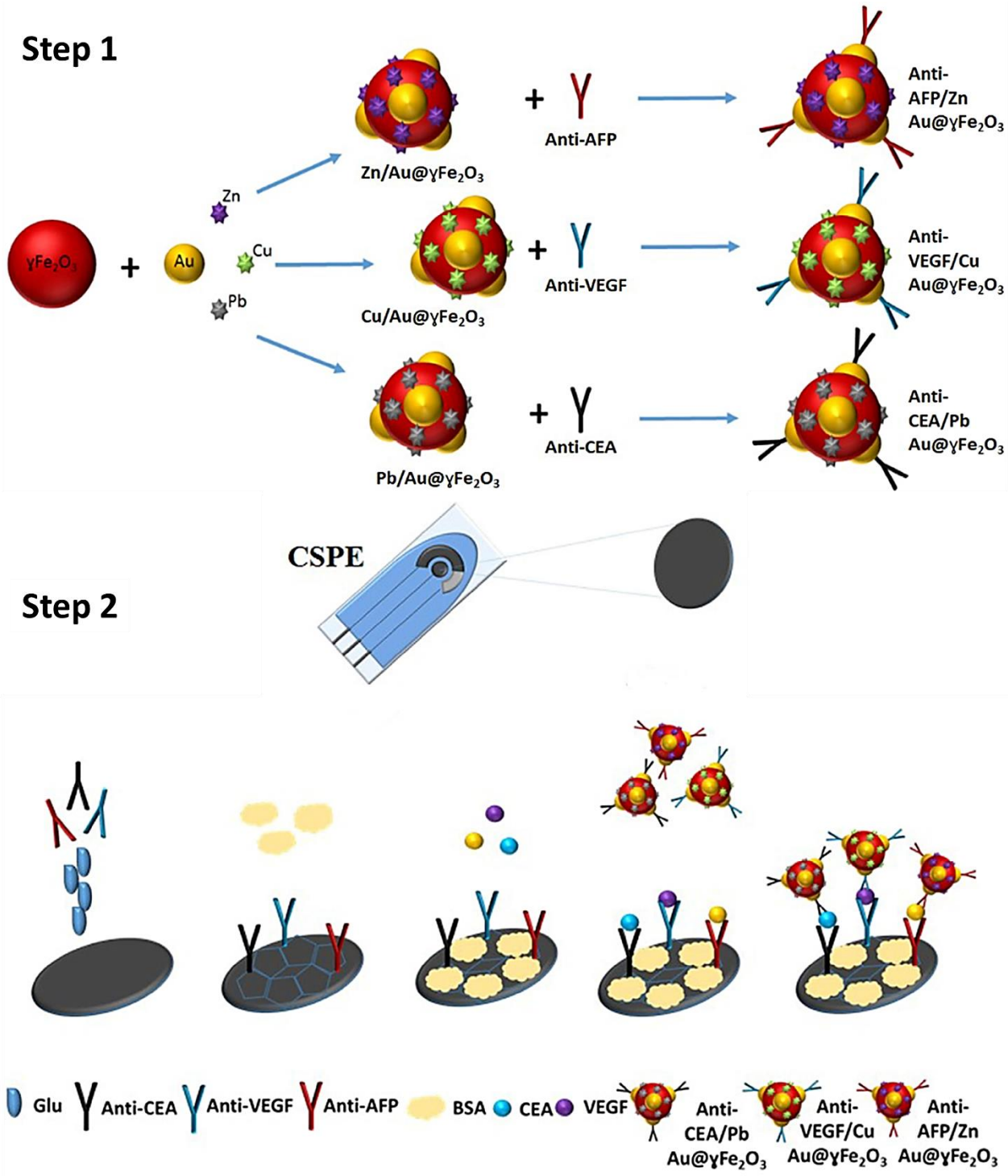

Fig. 4. A sketch of preparation and operation of the sandwich-type immunosensor for simultaneous determination of carcinoembryonic antigen (CEA), vascular endothelial growth factor (VEGF), and α-fetoprotein (AFP) biomarkers. (Reproduced with permission from Ref. [72]**)**.

Aptamer-based electrochemical sensors for cancer biomarkers

The early '90s witnessed the development of a new selection procedure for RNA sequences capable of selective binding of chosen target analytes of a non-nucleic acid nature. Two research groups, i.e., the Ellington and Szostak group [76], as well as the Tuerk and Gold group, independently came up with this procedure [77]. The SELEX name was given to this procedure as an abbreviation for the "systematic evolution of ligands by exponential enrichment." The resulting RNA sequences were called "aptamers" from the Latin word "aptus" (fit) combined with the Greek word "meros" (part). Later, the research was extended to DNA libraries [78]. With the SELEX, the formation of RNA or single-stranded DNA (ssDNA) aptamers from randomized RNA or DNA libraries is accomplished in three steps, i.e., forming the complex, separating unbound sequences, and amplifying the selected sequence aptamers. The sequences library and the target analyte are incubated to form the complex under optimized conditions. Next, the unbound sequences are filtered out, and the complex ones are amplified and then prepared for the next round. After several selection rounds, the obtained aptamers are cloned and stored under appropriate conditions [79]. One of the most exciting advantages of generating selective aptamers for cancer biomarkers is that the SELEX enables the selection of biological media, such as body fluids and tissues. SELEX is essential because it does not require advanced biochemical information about the selected target. However, intensive and careful counter-selection steps are necessary for eliminating non-specific recognizing sites [80].

Nowadays, aptamers are promising alternatives to antibodies. They are extensively used in designing novel biosensors for cancer biomarkers due to their numerous advantages, including high target affinity comparable to or even higher than antibodies. Moreover, they can recognize different forms and isoforms of proteins. Due to facile labeling, conjugation, and easy chemical modification, aptamers are primary candidates for use as biorecognition units in fabricating EC aptasensors for cancer biomarkers. Similar to immunosensors, one of the essential factors in fabricating EC aptasensors for cancer biomarkers is the immobilization of aptamers. Aptamers can be attached to the working electrode surface via the same ssDNA or double-stranded DNA (dsDNA) immobilization principle. The most popular strategies include physical adsorption, covalent bonding, chemisorption, and affinity-based immobilization, e.g., avidin-biotin interactions [81]. Similar to EC immunosensors, two modes in designing EC cancer biomarker

aptasensors have been reported: label-free and sandwich-type modes, the main difference being the replacement of antibodies with aptamers (Fig. 5).

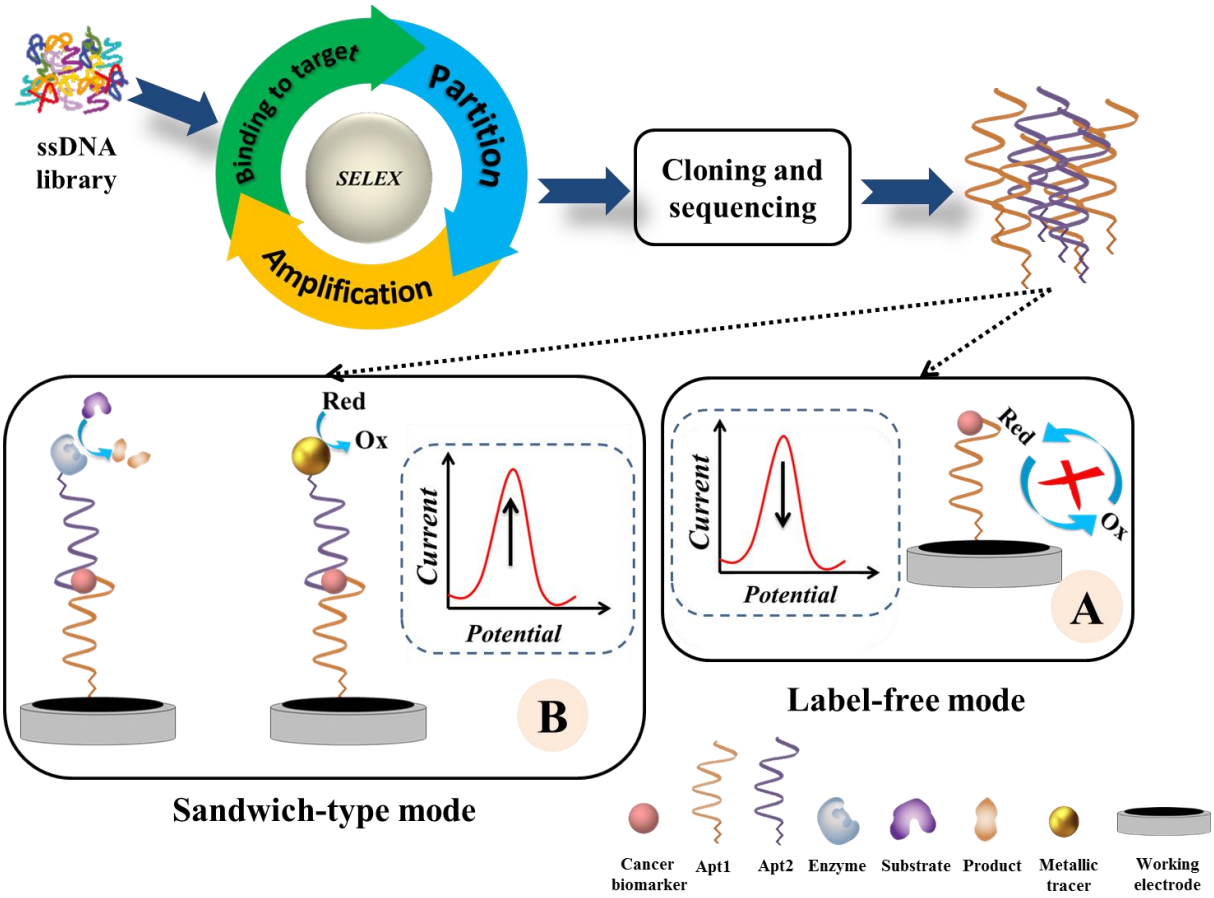

Fig. 5. The flowchart of an electrochemical cancer biomarker sensor preparation and operation based on aptamers as recognition units for both label-free and sandwich-type sensors.

Principle of the EC label-free aptamer-based sensors for cancer biomarkers

The design of a label-free EC aptasensor for a cancer biomarker is similar to that of an EC immunosensor. An EC signal can be amplified by employing functional nanomaterials to enhance the aptasensor response by facilitating electron transfer and decreasing the signal-to-noise ratio. The fabrication of a label-free EC aptasensor for a cancer biomarker generally requires a preliminary multistep modification of the electrode surface with nanomaterials, including metal and, notably, noble-metal (Au, Pt, Ag) NPs, carbon-based nanomaterials, including carbon

nanotubes (CNTs), graphene oxide (GO), and rGO, and transition metals (Cu, Zn, Fe) to improve the EC signal and increase the active surface area providing more active sites available for aptamers' immobilization [82]. After the successful immobilization of nanomaterials and aptamers on the electrode surface, the resulting aptasensor is immersed in the target cancer biomarker solution. Then, this biomarker is quantified by reading the change in the EC signal. This change is related to the affinity of the target biomarker and the aptamer [83] [84].

Electrochemical label-free aptasensors for cancer biomarkers

PSA was targeted by Jolly et al. [85] using an amperometric and impedimetric dual-mode aptasensor. To this end, 6-(ferrocenyl)hexanethiol or 6-mercapto-1-hexanol (MCH) was co-immobilized with PSA-specific DNA aptamers on the electrode, preliminary modified with AuNPs (Fig. 6); 6-(ferrocenyl) hexanethiol and MCH serving as the signal indicator for the amperometric and impedimetric determination, respectively. The LOD and the linear dynamic concentration range were 10 pg mL^{-1} and 10 pg mL^{-1} to 10 ng mL^{-1}, respectively; however, the interference study was not included to evaluate the selectivity. Methylene blue, used as the redox probe, is an important signal indicator in EC sensing non-electroactive targets, e.g., protein biomarkers. In a creative approach involving competitive interactions between complementary DNAs (cDNAs) and antigens, Raouafi et al. [86] devised a label-free aptasensor for PSA by trapping methylene blue between anti-PSA aptamers and cDNAs. In the presence of PSA and cDNAs, methylene blue was released, decreasing the DPV peak. The aptasensor precisely differentiated PSA from other analytes, including human serum albumin (HSA), CEA, and IgG. The linear dynamic concentration range and a LOD were 1 pg mL^{-1} to 100 ng mL^{-1} and 0.064 pg mL^{-1}, respectively.

Another unique strategy for selective EC enzyme-free aptasensing was developed for AFP [87]. The main idea was to recycle the AFP target analyte on the electrode surface to react with aptamers several times. That increased the sensitivity of the aptasensor. The sensor platform was prepared using graphene nanosheets followed by immobilizing AFP aptamers labeled with Prussian Blue NPs (PBNPs). After the introduction of AFP, the reaction between AFP and aptamers caused PBNPs to be released from graphene nanosheets, resulting in a free AFP-aptamer-PBNP complex. At this point, the role of deoxyribonuclease (DNase) comes for dissociating this complex to release AFP and react again with aptamer-PBNP. The DPV linear dynamic concentration range and the LOD were 0.01 to 300 ng mL^{-1} and 6.3 pg mL^{-1}, respectively.

As discussed above, in developing EC immunosensors, carbon nanomaterials, including rGO and CNTs, positively influence EC sensing, increasing the electrode's active surface area and electrical conductivity. Noble metals direct incorporation into carbon nanomaterials improved sensors' performance, including high catalytic activity and biocompatibility. Direct immobilization of HER2 aptamers on a GCE surface, preliminary modified with AuNPs/SWCNTs/rGO, resulted in a sensitive HER2 aptasensor. The EIS charge transfer resistance changes corresponded to the HER2 concentration changes. The aptasensor LOD and linear dynamic concentration range were 50 fg mL^{-1} and 0.1 pg mL^{-1} to 1 ng mL^{-1}, respectively. Moreover, it demonstrated a high discriminatory capability, ensuring it responds exclusively to the intended target in the presence of other proteins, including BSA, IgG, PSA, and thrombin [88]. Furthermore, another label-free aptasensor for CA 125 was devised with a decisive advantage: eliminating an external redox probe by directly modifying the working electrode surface with nickel hexacyanoferrate (NiHCF) to serve as a signaling probe. The sensing platform was further modified with polydopamine-functionalized graphene (PDA@GR) and aptamers. The sensor's LOD was 0.076 pg mL^{-1} with a linear DPV response of 0.10 pg mL^{-1} to 1.0 μg mL^{-1} [89].

As mentioned previously, the simultaneous determination of multiplexed biomarkers is very complicated to enable when dealing with the label-free mode; however, an innovative procedure was developed to simultaneously determine HER2 and estrogen receptor (ER) using a label-free aptasensor [90]. In this procedure, the aptamers are labeled with different electroactive tracers, namely Neutral Red (NB) and methylene blue (MB) for HER2 and ER, respectively. Then, the aptamers are immobilized on the working electrode surface. When the aptamer-biomarker complex is formed, it will be released from the electrode with the electroactive tracers (NB or MB), resulting in a decrease in their oxidation current signals, further quantified to attain a LOD of 3.8 fg mL^{-1} and 6.8 fg mL^{-1} for HER2 and ER, respectively.

Table 4. Electrochemical label-free aptamer-based sensors for cancer biomarkers.

Electrode modification	Target biomarker	Signal tranduction technique	Linear dynamic concentration range	Limit of detection	Number of interfering agents	Storage stability (days)	Ref.
AuE/AuNPs/thiolated Apt	PSA	SWV EIS	1 to 100 ng mL^{-1} 0.01 to 10 ng mL^{-1}	0.1 ng mL^{-1} 0.01 ng mL^{-1}	-	-	[85]
C-SPE/$GOCO_2H$/Apt/cDNA/MB	PSA	DPV	1 pg mL^{-1} to 100 ng mL^{-1}	0.064 pg mL^{-1}	3	14	[86]
GO-modified gold-disk electrode/PBNP-Apt	AFP	DPV	0.01 to 300 ng mL^{-1}	6.3 pg mL^{-1}	6	-	[87]
GCE/ErGO-SWCNT/AuNP/Apt	HER2	EIS	0.1 pg mL^{-1} to 1 ng mL^{-1}	50 fg mL^{-1}	6	30	[88]
C-SPE/PDA@Gr/NiHCF	CA 125	DPV	0.10 pg mL^{-1} to 1.0 μg mL^{-1}	0.076 pg mL^{-1}	-	-	[89]
ITO/(Zn-Co-MOF) (ZIF-8)/(Apt1-MB) Apt2-NB	HER2 ER	CV	0 to 15 pg mL^{-1}	3.8 fg mL^{-1} 6.8 fg mL^{-1}	-	-	[90]
Cd^{2+}-Apt@AMNFs@ZIF-67	HER2	EIS	0 to 1000 pg mL^{-1}	4.853 fg mL^{-1}	-	30	[91]
SiO_2/carboxyl functionalized photoresist-derived carbon/Apt	PDGF-BB	CV Capacitance EIS	0.005 to 50 nM	1.9 pM	3	10	[92]

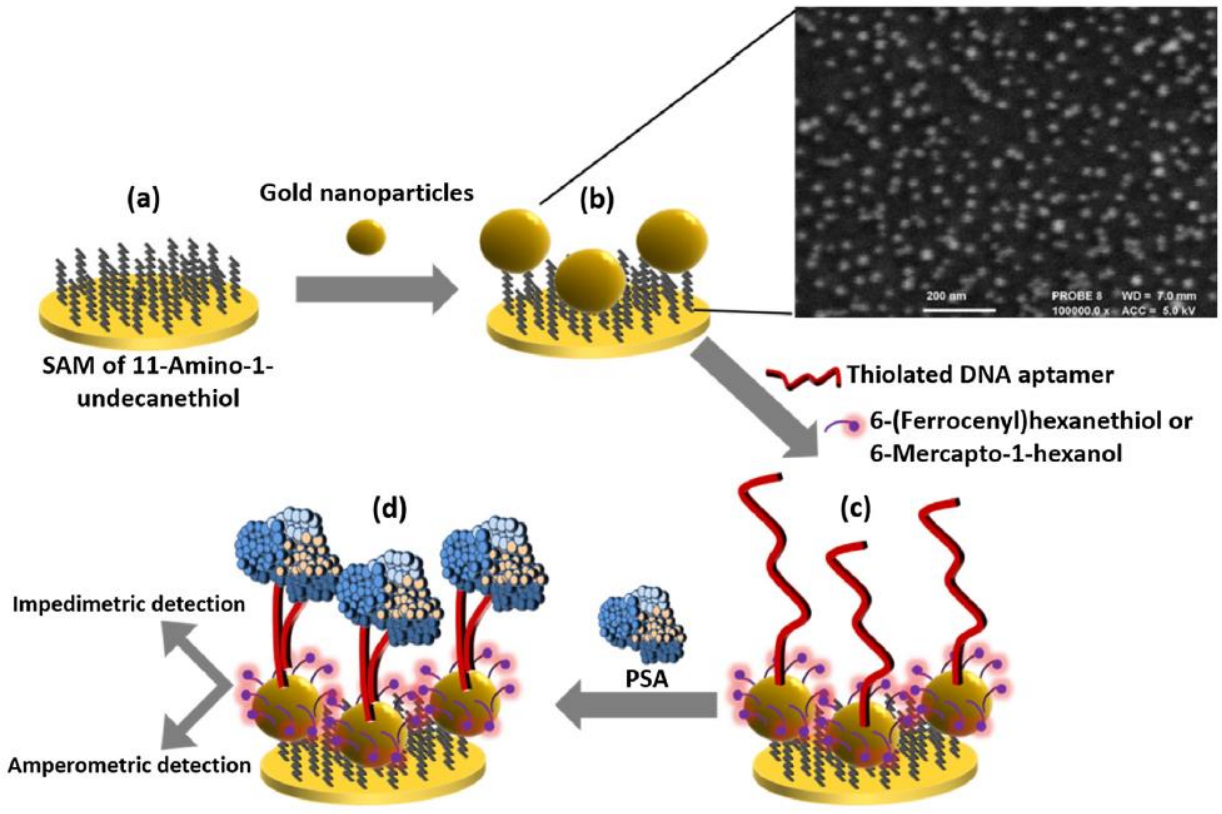

Fig. 6. The flowchart of self-assembling aptamers on gold nanoparticles followed by impedimetric and amperometric label-free determination of PSA. (Reproduced with permission from Ref. [85].)

Principle of the EC sandwich-type aptamer-based sensors for cancer biomarkers

Like EC immunosensors, aptasensors have also suffered from a lack of sensitivity, disabling them from reaching the application in real-world diagnosing and cancer monitoring. Inspired by the sandwich-type immunoassay design based on a pair of antibodies, researchers replaced this pair with a pair of aptamers to lift this limitation. In a typical EC sandwich-type aptasensor, the primary aptamer is immobilized on the electrode surface, preliminary modified with nanomaterials, and chemically functionalized for improving sensing performance. The secondary aptamers are attached to the signaling labels [93]. The sandwich is perpetuated by affinity interactions between antigens and aptamers in the presence of the target cancer biomarker. The quantification of the target is directly related to the generated signal from labels, proportional to the amount of the cancer antigen present.

Electrochemical sandwich-type aptasensors for cancer biomarkers

Different strategies were adopted for carcinoembryonic antigen (CEA) sensing. For instance, Shekari et al. [20] successfully used RNA-cleaving DNA enzyme (DNAzyme) with peroxidase-like catalytic activity to build a CEA aptasensor based on a sandwich-type amplification strategy. Graphene quantum dots (GQDs), AuNPs, and nitrogen-doped graphene were used for electrode modification to facilitate electron transfer and enlarge the electrode active surface area for a more stable primary aptamers' immobilization. The amplification label was prepared by bioconjugating secondary aptamers with DNAzyme using glutaraldehyde as the linker (Fig. 7). The aptasensor was catalytically highly active toward H_2O_2 electroreduction, traced with DPV for quantitive CEA determination. The linear dynamic concentration range and LOD were 10.0 fg mL^{-1} to 200.0 ng mL^{-1} and 3.2 fg mL^{-1}, respectively. The aptasensor operated with selective precision when detecting CEA in the presence of AFP, HSA, and CA 15-3.

Additionally, another unique strategy is enzyme inhibition amplification. It consists of catalyzing precipitation to form a precipitate-insulating film, gradually impeding the electron transfer. This strategy appeared fruitful in devising a sandwich-type aptasensor for CEA based on the HRP enzyme applied to catalyze precipitation of the product of the reaction between H_2O_2 and 4-chloro-1-naphthol(4-CN). For this amplification, two nanomaterials were synthesized. One was rGO

conjugated with AuNPs and hemin to form a platform for primary aptamers. The other was the organic-inorganic nanomaterial composed of AuNPs linked to HRP, with a nanoflower morphology, serving as the carrier for secondary aptamers. The CEA concentration increase increased the HRP concentration, increasing the amount of the precipitated film, which decreased the DPV peak signal. Its selectivity manifests itself with a decrease in false negative results when interfering with L-cysteine, thrombin, PSA, and hemoglobin; the linear dynamic concentration range and LOD being 100 fg mL^{-1} to 100 ng mL^{-1} and 29 fg mL^{-1}, respectively [94].

Recently, aptamers and antibodies were applied for CA 125 determination. Combining these recognition units in a single sensor leads to a hybrid affinity toward the target CA 125. Sadasivam et al. [95] modified a gold electrode with thiolated aptamers in this route. Then, antibodies were employed to prepare the amplification label using magnetic beads as carriers for antibodies and the HRP enzyme. Hybrid sensor affinity to CA 125 and catalytic activity in the presence of H_2O_2 as the external redox probe were high. CV and amperometry were used for CA 125 quantification, achieving the 0.08 U mL^{-1} LOD and the 2 to 100 U mL^{-1} linear dynamic concentration range. It is necessary to introduce direct interfering agents in addition to serum, as it is not discussed here relying solely on serum samples to assess selectivity comprehensively. In another study, a hybrid affinity-based receptor comprised of aptamer probes and antibodies explicitly tailored to the HER2 biomarker. The aptamer layer was immobilized on a gold electrode to serve as the primary receptor, and the antibodies enzyme was labeled as a signal reporter. Chronoamperometry showed a linear current response from 1 to 50 ng mL^{-1}, covering both normal and abnormal HER2 concentrations [96]. The hybrid approach harnesses antibodies' binding specificity and high aptamers' versatility, increasing sensitivity in detecting cancer biomarkers. However, aptamers' molecules are smaller and more flexible, making them better suited as labels for target capture, as reported by Jarczewska et al. [97], where they directly immobilized antibodies on a gold electrode and employed aptamers labeled with methylene blue as a capture probe for HER2. CV response revealed a low LOD of 0.001 ng·ml^{-1}. Both approaches, whether using antibodies or aptamers as labels, can be effective for the electrochemical detection of cancer biomarkers in a sandwich assay, displaying excellent selectivity when testing with different interfering agents.

Table 5. Electrochemical sandwich-type aptasensors for cancer biomarkers determining in serum.

Immunological Platform	Signal amplification probe	Signal tranduction technique	Target biomarker	Limit of detection	Linear dynamic concentration range	Number of interfering agents	Storage stability (days)	Ref.
GCE/GQD/AuNPs/NG/BSA/Apt1	Apt2/GA/Hemin–G4	DPV	CEA	3.2 fg mL^{-1}	10.0 fg mL^{-1} to 200.0 ng mL^{-1}	3	3	[20]
GCE/-rGO-AuNP/Hemin- Apt1	HRP-$Cu_3(PO_4)_2$HNF-AuNP-Apt2	DPV	CEA	29 fg mL^{-1}	100 fg mL^{-1} to 100 ng mL^{-1}	4	15	[94]
AuE/thiolated Apt	MBs/Ab/HRP	CV EIS	CA 125	0.08 U mL^{-1}	2 U mL^{-1} to 100 U mL^{-1}	-	-.	[95]
Aue/Apt	HRP/Ab	Amperometry chronoamperometry	HER2	1 ng mL^{-1}	1 to 100 ng mL^{-1}	6	-	[96]
Aue/Ab	MB/Apt	CV	HER2	0.001 ng mL^{-1}	0.01 to 10 ng mL^{-1}	5	-	[97]

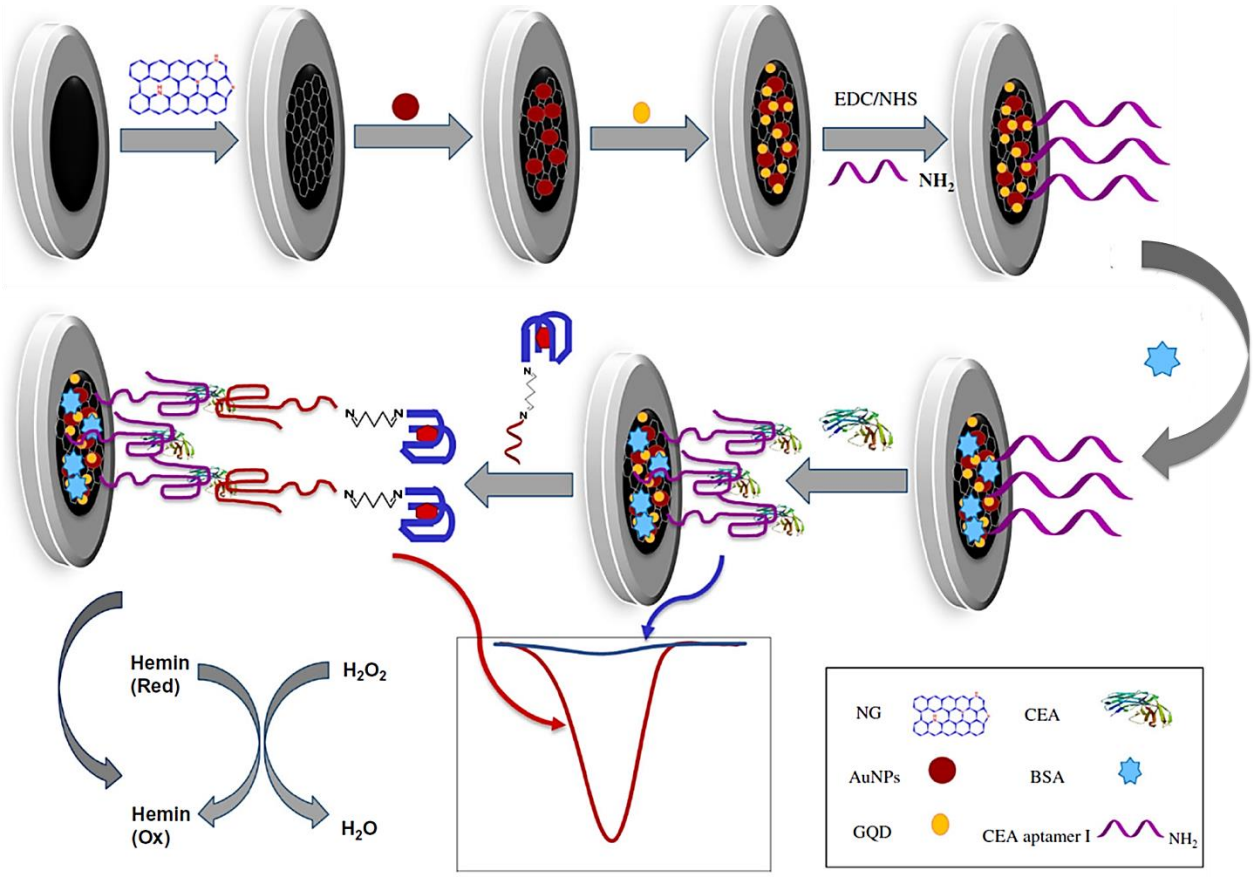

Fig. 7. The flowchart for carcinoembryonic antigen (CEA) determination with electrochemical sandwich-type aptasensor constructed using graphene quantum dots (GQDs), gold nanoparticles (AuNPs), and nitrogen-doped graphene (NG) modified electrode and exploiting the peroxidase-mimicking activity of a G-quadruplex DNAzyme. (Reproduced with permission from Ref. [20]).

The label-free and sandwich-type mode: Strengths and weaknesses

Cancer biomarker detection by electrochemical immunosensing and aptasensing operates through two immunoreaction modes: a label-free and a sandwich mode. In the sandwich mode, dual antibody, aptamer, or antibody-aptamer interactions are involved where the biomarker is captured between two recognition elements. The sandwich-type mode strongly affects the sensitivity by employing various signal amplification strategies that can be incorporated, such as enzyme-linked antibodies [98] or nanoparticles [99]; it also promotes specificity and reduces the likelihood of false positives by ensuring that both antibodies must bind to the target for detection. While signal enhancement is a key asset, complexities in procedures, higher reagent costs, and time-consuming steps pose challenges. In contrast, the label-free mode involves a single immunoreaction where the antibody or aptamer directly binds the target cancer biomarker, making the detection mechanism very simple and offering cost-effectiveness and real-time monitoring because of the absence of labeling agents, allowing for real-time monitoring of binding events, providing dynamic information about the interaction kinetics [100]. However, a lower sensitivity resulted because of the absence of the signal amplification probe and some concerns regarding the selectivity [101]. In addition, higher detection limits were reported compared to the sandwich-type mode. The right choice between these two modes depends on the unique detection requirements. Excelling in sensitivity and selectivity with sandwich-type mode while the label-free mode excels in simplicity and real-time insights. Consequently, researchers must strategically assess trade-offs to align their choice with desired sensitivity, selectivity, simplicity, and cost-efficiency in electrochemical immunosensor design.

Electrochemical molecularly imprinted polymer-based sensors for cancer biomarkers

MIPs are tailor-made synthetic polymers that can act as artificial receptors in EC sensors for the molecular recognition of target analytes with their selectively recognizing cavities; they are also called "plastic antibodies" for their ability to mimic these natural receptors [102]. In 1949, Dickey first reported in English about MIPs [103], which came with the key concepts we now use for preparing MIPs. Generally, the MIP preparation involves the formation of a pre-polymerization complex of the template with functional monomers in solution through covalent or non-covalent interactions. The analyte can serve as the template at this stage. Then, this complex is polymerized

in the presence of cross-linking monomers [104]. Non-covalent imprinting seems predominant, most commonly reported in MIP-based sensors for cancer biomarkers. After polymerization, the template is removed from the MIP. Extraction with an appropriate solvent is most frequently used [105]. This polymerization is accomplished using thermally- or (UV light)-induced polymerization, as well as emulsion, solution, suspension, and precipitation polymerization [106] [107] [108].

MIP synthesizing for cancer biomarkers determining

The MIP film synthesizing by traditional bulk solution polymerization using proteins or other biological macromolecular compounds as templates is challenging. That is because of hindered mass transport, the possibility of permanent template entrapment, inadequate film morphology, difficulties in finding the solvent appropriate for template extraction, and heterogeneous distribution of molecularly imprinted cavities featuring template-recognizing sites. Therefore, MIPs as recognition units for EC cancer biomarker sensors are prepared mainly by electropolymerization. That enables depositing conductive or non-conductive MIP films by functional and cross-linking monomers electropolymerizing in the template presence, depending on the EC technique for analyte determination and the desired sensing platform chosen, positively affecting the sensor's overall performance. Moreover, electropolymerization allows direct template imprinting in the MIP film deposited on the electrode surface, thus eliminating a time-consuming traditional template immobilization. This electropolymerization is most often performed under either potentiostatic or potentiodynamic conditions. The former requires a constant potential application, and the latter requires repeatable potential linear scanning over the potential range of either electroreduction or electro-oxidation of the functional and cross-linking monomers; the number of current-potential cycles and the potential scan rate control the resulting MIP film thickness and morphology. Thus, electropolymerization offers an attractive route for producing MIPs to determine proteins, including protein cancer biomarkers [109] [110]. The concept and the operation principle of an EC sensor for a cancer biomarker using the MIP recognition unit are illustrated in Fig. 8. Reaching sufficiently high detectability and reliability is required for applying a sensor in clinical determinations of those biomarkers. Besides, a sensor must accurately be assembled, MIP synthesis must carefully be optimized, monomers and template extracting solvents

must be selected suitably, the template must exhaustively be removed, and the analyte determination method must adequately be chosen.

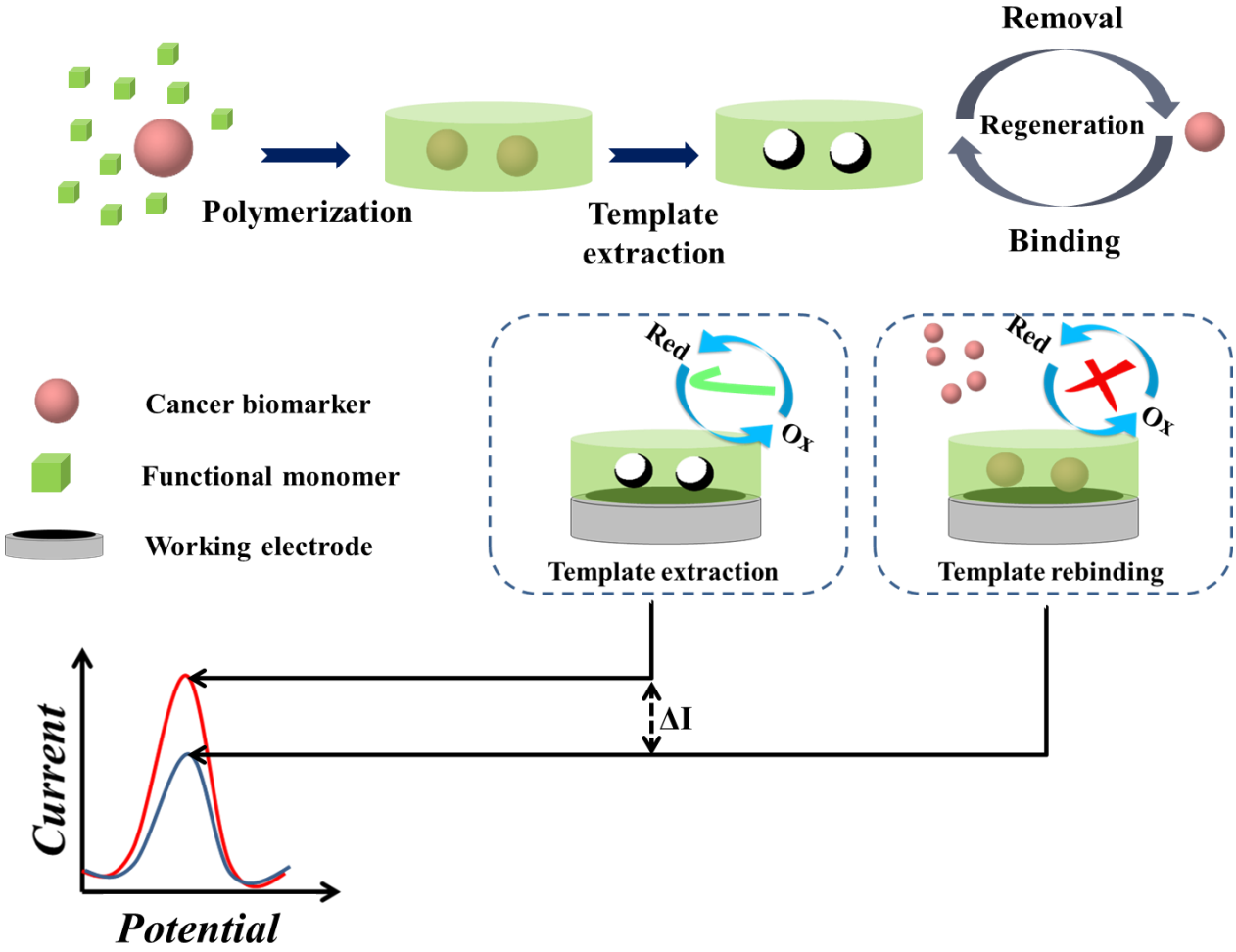

Fig. 8. Schematic illustration of preparing and operating a DPV sensor for a cancer biomarker using a molecularly imprinted polymer as the recognition unit.

Electrochemical MIP-based chemosensors for cancer biomarkers

Yazdani et al. [111] fabricated a MIP-based EC nano-biosensor for PSA. The imprinting was accomplished by electropolymerizing the pyrrole functional monomer in the presence of the PSA template. The in-solution self-assembled, then 24 h reacted PSA-pyrrole complex was next electropolymerized on the surface of the screen-printed gold electrode (Au-SPE). Then, after extracting the PSA template, DPV was used to investigate the sensing capability of the PSA sensor

with hexacyanoferrate as the redox probe (Fig. 9). The DPV linear dynamic concentration range was 0.01 to 4 ng mL^{-1} with a low LOD of 2.0 pg mL^{-1}. Noteworthy, however, selectivity tests were not carried out in this work. Similarly, Ma et al. [112] employed noble metals and carbon nanomaterials to enhance electron transfer and increase film porosity for a MIP-based sensor for PSA. The synthesized graphene sheets (GSs) and gold nanoparticles (GS-AuNPs) nanocomposite suspension were drop-cast on the surface of GCE. Chitosan was introduced to prevent any leakage. Finally, the MIP film was deposited by electropolymerization using dopamine as the functional monomer because of its biocompatibility. DPV demonstrated a wide linear dynamic concentration range of 1 pg mL^{-1} to 100 ng mL^{-1} PSA and a very low LOD of 0.15 pg mL^{-1}.

Moreover, the sensor substantiated its effectiveness for PSA determination in real serum samples and relied on specific binding interactions even in the presence of human immunodeficiency virus p24, hCG, AFP, CEA, and some ions that may be present in human serum as interfering agents. In the same context of PSA determination with an MIP-based EC chemosensor, Abbasy et al. [113] examined ways of decreasing MIP film degradation. They chose Toluidine Blue (TB) as the functional monomer and a pre-formed cysteamine-glutaraldehyde complex to construct an electrically conducting MIP film on the surface of the gold electrode. The DPV responses of the $Fe(CN)_6^{3-}/Fe(CN)_6^{4-}$ redox probe evidenced this device as a promising candidate for clinical use by covering a broad linear dynamic concentration range of 1 to 60 μg L^{-1} PSA, revealing a limit of quantification (LOQ) of 1μg L^{-1}. The selectivity tests were performed using CEA and HSA; however, using just two interfering agents falls short of performing a comprehensive selectivity assessment.

Furthermore, Lai et al. [114] targeted AFP determination with an MIP-based sensor. Toward that, they modified GCE with PTh-AuNPs. The AFP template was imprinted in a polymer via dopamine electropolymerization. After template extraction, selective molecular cavities were vacated in the MIP. The sensor performance was outstanding, demonstrated by a wide linear dynamic concentration range of 0.001 to 800 ng mL^{-1} AFP and a low LOD of 0.8138 pg mL^{-1}. Moreover, the sensor satisfactorily determined AFP in a selective manner tested against dopamine, ascorbic acid, uric acid, CEA, and human serum samples.

Additionally, Pacheco et al. fabricated an MIP-based EC sensor to determine CA 15-3 [115], achieving a DPV linear dynamic concentration range of 5 to 50 U mL^{-1} and a LOD of 1.5 U mL^{-1}.

The MIP film was prepared in two steps. First, CA 15-3 was adsorbed onto an Au-SPE. Then, an MIP framework was grown via electropolymerization around the adsorbed template molecules employing 2-aminophenol as the functional monomer. The exciting issue about this study is the choice of interfering agents, where HER2-ECD and cystatin C were selected. That was because their molecular sizes were smaller than CA 15-3. Therefore, they can penetrate the imprinted cavities, and HER2-ECD revealed a strong interfering effect, resulting in a low selectivity toward CA 15-3. Ribeiro et al. [116] proposed another CA 15-3 sensing strategy with the MIP EC sensor. They minimized the MIP film degradation by modifying the Au-SPE with tailed TB, electropolymerized in the presence of the CA 15-3 template. The resulting conductive poly(TB) significantly enhanced the sensor sensitivity and stability, reaching a LOD of 0.10 U mL^{-1} and a wide linear dynamic concentration range of 1 to 100 U mL^{-1}.

Furthermore, Gomes et al. studied three different amine-substituted benzene ring compounds, vis., *o*-phenylenediamine, *p*-phenylenediamine, and aniline, as functional monomers [117]. They introduced a new determination procedure involving the CA 15-3 template labeling with charges. After optimization, *o*-phenylenediamine was selected as the most appropriate functional monomer to prepare a (CA 15-3)-imprinted polymer by electropolymerization. The charged species presence (4-styrene sulfonic acid sodium salt negatively and dopamine positively charged) improved the sensor's performance, demonstrated by a low LOD of 0.05 U mL^{-1} and a linear dynamic concentration range of 0.25 to 10.00 U mL^{-1}. However, both of the last CA 15-3 MIP-based sensors reported only the serum sample tests, and as we discussed above, a robust examination of selectivity necessitates the introduction of direct interfering agents. In the same context, polypyrrole, a widely used conductive polymer, was also considered for surface imprinting of CA 15-3. Pyrrole was directly electropolymerized around the CA 15-3 template molecules adsorbed on the surface of the fluorine-doped tin oxide (FTO) electrode. A linear dynamic concentration range and a LOD of the DPV sensor were 1.44 to 13.2 U mL^{-1} of 1.07 U mL^{-1} [118]. For this study, CEA and IL-6 were selected for the cross-interfering tests, and a high selectivity was reached, although only two interfering agents provided a limited representation of potential interference scenarios.

Also, CEA was used as the template and a target for fabricating an MIP EC sensor. Moreira et al. [119] used an Ag-SPE as the substrate for the MIP film deposition to achieve high electric

conductivity. The CEA imprinted polymer was prepared by pyrrole electropolymerizing in the CEA template presence. Then, the template was extracted with proteinase K from the resulting MIP, and then the sensor was tested with CV, EIS, and SWV. CV afforded the broadest linear dynamic concentration range, i.e., 0.05 to 1.25 pg mL^{-1}. The selectivity was demonstrated using myoglobin and creatinine as interfering agents in addition to serum samples; however, the LOD was not reported.

Moreover, Shen et al. [120] fabricated an ultrasensitive DPV sensor for human chorionic gonadotropin (hCG) using an MIP as the selective recognition unit. To this end, a GCE was coated with chitosan, MWCNTs, and glutaraldehyde to bind the hCG template covalently. Then, the MIP film was deposited by electropolymerization using dopamine as the functional monomer, followed by template extraction. This sensor LOD of 0.5 pg mL^{-1} was low, but the linear dynamic concentration range of 0.5 to 250 ng mL^{-1} was ultra-wide. Different interfering agents with different sizes were used to evaluate the selectivity, including CEA (180 kDa), AFP (66 kDa), HIV-p24 (24 kDa), and cTnI (22 kDa). It can be concluded that compounds of molecules bigger than the template are readily excluded from the cavity in contrast to small molecules, which can cause some interfering effects.

Besides, In a comparative study, Rebelo and coworkers demonstrated that EC sensing is highly sensitive and cost-effective [121]. They measured responses of SWV and surface plasmon resonance (SPR) spectroscopy, used as an optical technique, for CA 125 determination. Two MIP-based sensors were fabricated by electropolymerization of pyrrole on the surface of the Au-SPE. The EC sensor's performance was higher than the SPR sensor's, reaching an SWV LOD of 0.01 U mL^{-1} and a linear dynamic concentration range of 0.01 to 500 U mL^{-1}. The interference study to examine the selectivity was performed only with artificial serum; nevertheless, high selectivity was achieved.

In addition, Bozal-Palabiyik et al. [122] developed a simple single-step procedure for the impedimetric determination of vascular endothelial growth factor (VEGF). They determined VEGF at a low, i.e., pictogram level. The sensor exploited a VEGF-templated MIP film prepared by electropolymerization of *o*-phenylenediamine on the surface of the C-SPE. The sensor's linear dynamic concentration range was wide, extending from 20 to 200 pg mL^{-1} VEGF, and the LOD was low, equaling 0.08 pg mL^{-1}. Moreover, the sensor demonstrated appreciable performance in

determining VEGF in human serum samples, and a low interfering effect was noticed with HER2, CA 125, and PSA, revealing its high selectivity.

Cancer biomarkers with low-molecular-weight compounds were also targeted by EC MIP-based sensors. For the EC selective determination of pyruvic acid (PA), an essential metabolite-based cancer biomarker, two functional monomers, vis., methacrylic acid (MA) and ethylene glycol dimethacrylate (EGDMA), were copolymerized in the presence of PA. Then, the sensing platform was supported with CNTs to enhance the DPV signal by increasing the electrode's active surface area. The devised MIP chemosensor linear dynamic concentration range of 0.1 to 200 µM was appreciable, and the LOD was 0.048 µM. Moreover, PA recovery in urine and plasma samples was high, with excellent selectivity tested against citric acid, ascorbic acid, lactic acid, tartaric acid, and oxalic acid [123]. Following the molecular imprinting strategy, we have recently devised a CV sensor for lactic acid (LA), a small-molecule critical agent for screening malignant cells in stage II or stage III cancer [124]. The MIP film was prepared by electropolymerization of aniline in the presence of the LA template on the surface of a gold electrode, preliminary modified with green-synthesized rGO and AgNPs. The chemosensor allowed us to reach the LOD of 0.72 µM LA with long stability and high selectivity examined using different interfering agents.

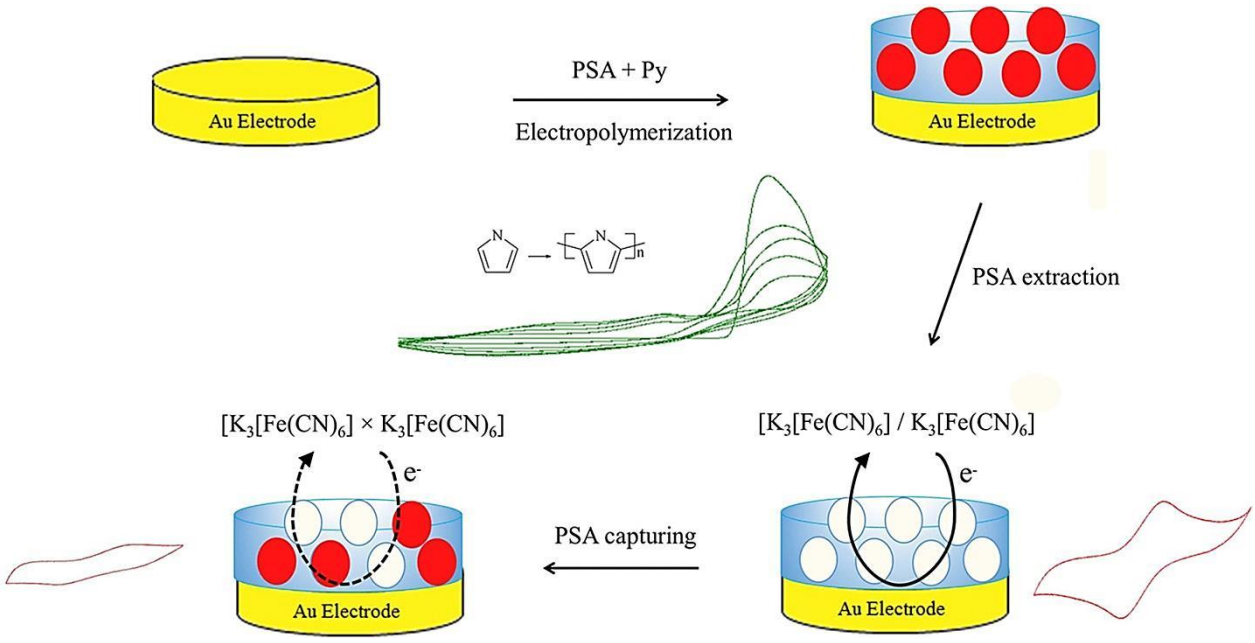

Fig. 9. The flowchart for preparing and operating an electrochemical molecularly imprinted polymer sensor for PSA determination. (Reproduced with permission from Ref. [111]).

Table 6. Electrochemical MIP-based sensors for cancer biomarkers.

Sensor composition	Functional monomer	Template biomarker	Polymerization method	Signal tranduction technique	Linear dynamic concentration range	Limit of detection	Number of interfering agents	Storage stability (days)	Ref.
Au-SPE/MIP	Pyrrole	PSA	Electropolymerization	DPV	0.01 to 4 ng mL^{-1}	2.0 pg mL^{-1}	-	6	[111]
GCE/GS-AuNP/CS/MIP	Dopamine	PSA	Electropolymerization	DPV	1 pg mL^{-1} to 100 ng mL^{-1}	0.15 pg mL^{-1}	8	14	[112]
AuE/cysteamine/GA/MIP	Toluidine Blue	PSA	Electropolymerization	DPV	1 to 60 µg L^{-1}	1 µg L^{-1}	2	14	[113]
GCE/AuNPs/PTh/ MIP	Dopamine	AFP	Electropolymerization	DPV	0.001 to 800 ng mL^{-1}	0.8138 pg mL^{-1}	4	30	[114]
Au-SPE/MIP	2-Aminophenol	CA 15-3	Electropolymerization	DPV	5 to 50 U mL^{-1}	1.5 U mL^{-1}	2	-	[115]
Au-SPE/glutaraldehyde/AOT/ MIP	Toluidine Blue	CA 15-3	Electropolymerization	DPV	0.10 to 100 U mL^{-1}	0.10 U mL^{-1}	-	-	[116]
Au-SPE/MIP	*o*-Phenylenediamine	CA 15-3	Electropolymerization	CV	0.25 to 10.00 U mL^{-1}	0.05 U mL^{-1}	-	-	[117]
FTO/MIP	Pyrrole	CA 15-3	Electropolymerization	Potentiometry	1.44 to 13.2 U mL^{-1}	1.072 U mL^{-1}	2	14	[118]
Ag-SPE/MIP	Pyrrole	CEA	Electropolymerization	CV, EIS, and SWV	0.05 to 1.25 pg mL^{-1}	1pg mL^{-1}	2	-	[119]
GCE/GA/CS/MWCNTs/MIP	Dopamine	hCG	Electropolymerization	DPV	0.5 pg mL^{-1} to 250 ng mL^{-1}	0.035 pg mL^{-1}	4	15	[120]
Au-SPE/MIP	Pyrrole	CA 125	Electropolymerization	SWV	0.01 to 500 U mL^{-1}	0.01 U mL^{-1}	-	-	[121]
G-SPE/MIP	*o*-Phenylenediamine	VEGF	Electropolymerization	EIS	20 to 200 pg mL^{-1}	0.08 pg mL^{-1}	4	-	[122]
CNT-CPE/MIP	MAA and EGDMA	Pyruvic acid	precipitation polymerization	DPV	0.1 to 200 mM	0.048 µM	5	180	[123]
AuE/rGO-AgNPs/MIP	Aniline	Lactic acid	Electropolymerization	CV	10 to 250 µM	0.726 µM	5	-	[124]
Au-SPE/MIP	Phenol	HER2-ECD	Electropolymerization	DPV	10 to 70 ng m L^{-1}	1.6 ng L^{-1}	2	-	[125]
GCE/AuNPs/PTh-MIP	Dopamine	CEA	Electropolymerization	DPV	0.001 to 1000 ng mL^{-1}	0.2589 pg mL^{-1}	4	30	[126]
GCE/MIP	*o*-Phenylenediamine	Cys	Electropolymerization	CV	0.1 to 20 nM mL^{-1}	0.333 pM mL^{-1}	9	10	[127]
	o-Phenylenediamine	Cys	Electropolymerization	CV	0.1 to 20 nM mL^{-1}	0.333 pM mL^{-1}			
	o-Phenylenediamine	NADPH	Electropolymerization	CV	0.06 to 20 nM mL^{-1}	0.2 pM mL^{-1}			
	o-Phenylenediamine	$NADP^+$	Electropolymerization	CV	0.06 to 20 nM mL^{-1}	0.2 pM mL^{-1}			
SPE/MIP+Label probe for PSA: Ab-GO-MWCNT-Fe_3O_4	AAM and NNMBA	PSA	Precipitation polymerization	EIS	0.01 to 100 ng mL^{-1}	5.4 pg mL^{-1}	9	45	[128]
		Myo			1 to 20000 ng mL^{-1}	830 pg mL^{-1}			
C-SPE/AuNPs/MIP	Aminothiophenol	Sarcosine	Electropolymerization	EIS	0.011 to 17.9 µM	8.5 nM	2	7	[129]

DSP-SPE/MIP Label probe for dual determination AbEGFR-Cd(II)@LP AbVEGF-Cu(II)@LP	AAM	EGFR VEGF	Electropolymerization	DPV	0.05 to 50000 pg mL^{-1} 0.01 to 7000 pg mL^{-1}	0.01 pg mL^{-1} 0.005 pg mL^{-1}	9	60	[130]
GCE/MIP	*p*-Aminobenzeneboronic acid	poly-sialic to capture CD56	Electropolymerization	DPV	10 to 150 ng L^{-1}	0.47 ng L^{-1}	9	3	[131]
SPE/ZnO Nanorods/MIP	Ethylene-co-vinyl alcohol	NMP22	Bulk polymerization	CV	1.0 to 1000 pg mL^{-1}	1.0 pg mL^{-1}	4	-	[132]
C-SPE/Nafion/Ni(OH)/MWCNT/MIP	2-Acrylamido-2-methyl-1-propanesulfonic acid and 4-vinylpyridine TRIM (crosslinker) AIBN (free-radical initiator)	Sarcosine	Bulk polymerization	CV	3.20 to 25.00 µM	0.96 µM	4	-	[133]
GCE/poly[(Cys)VIMBF$_4$]/AuNPs/MIP	1-[3-(*N*-cystamine)propyl]-3-vinylimidazolium tetrafluoroborate ionic liquid	AFP	Bulk polymerization	DPV	0.03 to 5 ng mL^{-1}	2 pg mL^{-1}	7	7	[134]
GCE/MIP	MA EGDMA AIBN initiator	Sarcosine	Precipitation polymerization	DPV	5.0 µM to 1.1 mM	0.38 µM	8	-	[135]
AuE/AuNPs-MIP	Scopoletin	NSE	Electropolymerization	SWV	25 to 4000 pg mL^{-1}	25 pg mL^{-1}	-	-	[136]
GCE/MIP	*o*-Phenylenediamine	double epitope epitope glycosyl for capturing CA 19-9	Electropolymerization	DPV	Polysaccharide imprinted sensor 0.1 to 5 U mL^{-1} Monosaccharide imprinted sensor 1 to 50 U mL^{-1}	0.028 U mL^{-1} 0.17 U mL^{-1}	9	3	[137]
GCE/AuNPs-GO/ MIP+label probe SiO_2@Ag/dsDNA/RhB	Nafion, MAA, AIBN and EGDMA	RhB for capturing BRCA 1	Free radical polymerization	DPV	10 fM to 100 Nm	2.53 fM	3	30	[138]
GCE/CS/GA/MIP	AAm MBA APS	AFP	Surface imprinting	DPV	8.0×10^{-4} to 10 µg mL^{-1}	0.096 ng mL^{-1}	3	14	[139]
GCE/MoS_2/AuNPs/MPBA/MIP and Au-PMB/MPBA as a tracing tag	*o*-Phenylenediamine-3-aminophenylboronic acid	PSA	Electropolymerization		10^{-4} to 10^4 ng mL^{-1}	0.03 pg mL^{-1}	7	35	[140]
CNTE/AuNPs/MIP	*o*-Phenylenediamine	CA 15-3	Electropolymerization	DPV	-	-	-	-	[141]

Cancer biomarker sensing merits and applications

The main goal of devising new analytical tools and developing new procedures for cancer biomarkers is the rapid, cost-effective, and accurate identification and quantification of these bioanalytes in body fluids. Among the first EC sensors for cancer biomarkers were immunosensors using natural antibodies as recognition units. However, several technical and economic limitations arise from the antibodies' fragility and relatively high costs. Therefore, many efforts have been put into overcoming these limitations to reach higher performance at a lower cost. Tables 2 - 6 summarize current strategies for EC sensing of cancer biomarkers using the three main recognition units, i.e., antibodies, aptamers, and MIPs. Crucial factors to be considered when evaluating the analytical performance of sensors, i.e., the LOD, linear dynamic concentration range, selectivity, and a real-sample test, are herein discussed for all types of above EC sensors.

The LOD is a crucial analytical parameter expressing sensor detectability. It must be very low if determining trace amounts of cancer biomarkers circulating in body fluids. All types of sensors discussed above met this prerequisite, reaching the required LOD values. Advantageously, the lowest LOD of 12 fg mL^{-1} was reported for CEA determination using a sandwich-type antibody EC sensor. The adopted sensing strategies included using nanomaterials to enhance the analytical signals and different strategies, such as the label-free and the sandwich-type modes. The method optimization and innovation introduced in these EC devices can remarkably increase the assay sensitivity toward cancer biomarkers determination.

The primary role of the recognition unit is selectivity, which is essential in commercializing EC cancer biomarker sensors. The recognition unit must provide high selectivity, especially in complex matrices, e.g., human body fluids. Applying nucleic acid- and protein-containing recognition units is more common to reach maximum selectivity. EC antibody-comprising cancer biomarker immunosensors have widely been investigated as point-of-care testing (POCT) devices. Aptamers have emerged in scientific research, gaining much interest as synthetic recognition units, especially in cancer biomarkers determination. Although MIPs are still not typical in the market of sensors for cancer biomarkers, they revealed a strong potential as a replacement for antibodies and aptamers due to their physical and chemical stability, low cost, and simplicity in preparation. Recent developments in fabricating sensors for cancer biomarkers demonstrated that MIPs are very

selective and can serve as attractive recognition units for sensing applications. That advantageously reveals a high to excellent selectivity toward these biomarkers. As evidenced by the data in Tables 2 - 6, the quantitative impact of the number of interfering agents is profoundly significant, as it substantially influences the sensor's performance and reliability. The number of interfering agents for the antibody-based sensing platforms was between 3 and 10, for aptamer between 3 and 6, and for MIPs between 2 and 9, although some reports did not discuss the number of interfering agents or used serum samples, assuming that it includes different compounds. However, the direct interfering effect with known agents and an excessive concentration will give solid data about the sensor's selectivity. Bio- and chemosensors for cancer biomarkers, characterized by diminished selectivity, are at risk of yielding erroneous results, either by generating false positives or negatives, because of non-specific interactions with interfering species. Thus, the meticulous design and optimization of recognition elements must, in essence, prioritize the minimization of interference stemming from non-target compounds. An enhanced focus on selectivity guarantees the precision of cancer biomarker quantification and, possibly more critically, bolsters the overarching efficacy of these electrochemical sensors in the intricate landscape of clinical diagnostic applications.

Repeatability is used to investigate the precision and accuracy of the sensor, measuring the signal variation under the same experimental conditions using the same sensor in a short time, while reproducibility measures the analytical signal variation between different sets of sensors prepared using the same procedure. Therefore, reproducibility is a more potent precision and accuracy indicator, expressing its usefulness as a POCT device [142]. Most reported EC sensors for cancer biomarkers (Tables 2 - 6) investigated neither reproducibility nor repeatability. However, those should be tested before releasing the sensor from the laboratory. The precision can be affected by many factors, e.g., the amount of immobilized antibody or aptamer, non-uniformity of the MIP surface, and the amount of the deposited labeling probe in the sandwich-type sensing mode. Nevertheless, molecular imprinting in polymers ensures a stable preparation procedure. That is reached by decreasing the manual intervention due to direct MIP film deposition by electropolymerization, thus leading to higher precision. Therefore, extensive laboratory investigations must validate the determination protocol and working conditions to apply a new sensing device in the biomedical field.

One of the primary roles in sensor commercialization is storage stability. The sensor response should be constant over a long time, enabling its storage. The storage stability of the discussed EC sensors was considered, and only a few survived two months of storage (Tables 2 - 6). Various factors can affect the storage life, including the type of recognition unit, nanomaterials applied for electrode modification, type of signaling labels, recognition unit deposition strategy, and chemical interactions. Storage stability of MIP-based EC sensors for cancer biomarkers is longer than that of antibody- and aptamer-based sensors, reaching up to 180 days for PA sensors. That results from the fragility of aptamers' antibodies and DNA strains (Tables 2 – 6).

Multiplexed cancer biomarkers determination can be advantageous because some cancers must be diagnosed using several biomarkers to confirm the malignancy. Therefore, devising different EC sensors for different biomarkers of the same tumor would allow for a single-step simultaneous determination of cancer biomarkers in the same sample. The strategy of simultaneous determination can be applied in the sandwich-type mode (Table 3). This strategy aims to differentiate the generated signals by tagging the detection probes with different labels and quantifying each cancer biomarker separately; it is also applicable if using aptamers. However, there is no report about using MIPs for the simultaneous EC determination of cancer biomarkers with the sandwich-type mode.

On-site determination is crucial for the biomedical application and commercialization of sensors. Most EC sensors for cancer biomarkers determination require a long pretreatment time to complete the interaction between the target analyte and the sensor recognition unit. The maximum pretreatment time acceptable for commercializing a sensing device is between 15 and 20 min. Furthermore, EC sensing can enable miniaturization and the portability of sensing devices by employing microfluidic chips and smartphones that can be programmed to measure detection signals.

Table 7. Comparison of properties of antibodies, aptamers, and molecularly imprinted polymers used as recognition units in electrochemical sensors for cancer biomarkers.

Feature		Antibody	Aptamer	Molecularly imprinted polymer
Fabrication method		Animal immune response	SELEX procedure	Molecular imprinting
Preparation time		>6 months	Few months	Few minutes to few hours
Amount of target analyte needed		Medium	High	High
Number of monomers available		~20 (amino acids)	>1000	>1000
Functionalization possibility		Low	Medium	High
Storage time		Short	Medium	Long
Thermal stability		Low	Low	High
pH stability		Low	Low	High
Stability against organic solvents		Low	Low	High
Immunogenicity		High	Low	-
Binding affinity	Small molecules	Low	Moderate	High
	Large molecules	High	High	High
Selectivity	Small molecules	Low	High	High
	Large molecules	High	High	Low
Cost		High	Medium	Low
Regeneration possibility		Low	Medium	High

Conclusions

Devising, fabricating, and testing EC sensors for cancer biomarkers have attracted great interest because of EC techniques' rapidity, portability, and low cost. Rapid clinical determination of cancer biomarkers for disease diagnosing and monitoring is a critical factor that can directly affect patient outcomes. In the present article, the classification of recent advances in EC sensors for cancer biomarkers based on the used recognition unit falling into three categories, vis., antibody, aptamer, and MIPs-based sensors, has extensively been reviewed. "Plastic antibodies," the name given to aptamers and MIPs whose engineered biomimetics selectively recognize target analytes, have attracted much attention, offering a low cost-to-performance ratio, an essential advantage toward commercialization. However, EC aptamer-based sensors for cancer biomarkers are less frequent than MIP- and antibody-based. Almost every original publication on MIPs starts by

claiming that under harsh environmental conditions, MIPs as receptors are more stable than biomacromolecules, as demonstrated in the present review. MIPs outperform aptamers and antibodies regarding resistance to pH and temperature changes and stability against organic solvents (Table 7). Concerning selectivity, after analyzing all types of (cancer biomarker)-sensing receptors, the overall conclusion is that aptamers are more selective than antibodies and MIPs. That is related to the aptamer nature, which is more suitable for both large and small target analyte molecules, but more reports on aptamer sensors are needed to confirm these results univocally. The storage time of all sensors was herein discussed, and, expectedly, the longest time was reported for MIP-based sensors. In contrast, the shortest times were for antibody-based sensors because of the antibodies' fragility. One of the significant limitations of MIP-based sensors is to differentiate each EC current signal for a given target to enable simultaneous determination. Multiplexing determination of cancer biomarkers can offer an essential advantage because some cancers must be diagnosed using different biomarkers to confirm the malignancy. Therefore, new approaches and preparation methods are needed, including the receptors' hybridization using aptamers and MIPs in a sandwich-type EC sensor [143], offering a breakthrough toward simultaneous determinations.

Acknowledgments

WK acknowledges the National Center for Research and Development of Poland for financial support through Grant No. SensIPF PL-TW/VI/2/ 2019.

References

[1] Cancer, (n.d.). https://www.who.int/news-room/fact-sheets/detail/cancer (accessed February 21, 2023).

[2] L. Wang, Q. Xiong, F. Xiao, H. Duan, 2D nanomaterials based electrochemical biosensors for cancer diagnosis, Biosens. Bioelectron. 89 (2017) 136–151. https://doi.org/10.1016/j.bios.2016.06.011.

[3] Y.-E. Choi, J.-W. Kwak, J.W. Park, Nanotechnology for Early Cancer Detection, Sensors. 10 (2010) 428–455. https://doi.org/10.3390/s100100428.

[4] L. Xing, N.W. Todd, L. Yu, H. Fang, F. Jiang, Early detection of squamous cell lung cancer in sputum by a panel of microRNA markers, Mod. Pathol. 23 (2010) 1157–1164. https://doi.org/10.1038/modpathol.2010.111.

[5] N.L. Henry, D.F. Hayes, Cancer biomarkers, Mol. Oncol. 6 (2012) 140–146. https://doi.org/10.1016/j.molonc.2012.01.010.

[6] B. Mohan, S. Kumar, H. Xi, S. Ma, Z. Tao, T. Xing, H. You, Y. Zhang, P. Ren, Fabricated Metal-Organic Frameworks (MOFs) as luminescent and electrochemical biosensors for cancer biomarkers detection, Biosens. Bioelectron. 197 (2022) 113738. https://doi.org/10.1016/j.bios.2021.113738.

[7] N. Mohajeri, E. Mostafavi, N. Zarghami, The feasibility and usability of DNA-dot bioconjugation to antibody for targeted in vitro cancer cell fluorescence imaging, J. Photochem. Photobiol. B. 209 (2020) 111944. https://doi.org/10.1016/j.jphotobiol.2020.111944.

[8] G. Kabay, J. DeCastro, A. Altay, K. Smith, H. Lu, A.M. Capossela, M. Moarefian, K. Aran, C. Dincer, Emerging Biosensing Technologies for the Diagnostics of Viral Infectious Diseases, Adv. Mater. 34 (2022) 2201085. https://doi.org/10.1002/adma.202201085.

[9] Y. Tao, F. Luo, Y. Lin, N. Dong, C. Li, Z. Lin, Quantitative gold nanorods based photothermal biosensor for glucose using a thermometer as readout, Talanta. 230 (2021) 122364. https://doi.org/10.1016/j.talanta.2021.122364.

[10] F. Arshad, F. Nabi, S. Iqbal, R.H. Khan, Applications of graphene-based electrochemical and optical biosensors in early detection of cancer biomarkers, Colloids Surf. B Biointerfaces. 212 (2022) 112356. https://doi.org/10.1016/j.colsurfb.2022.112356.

[11] D.R. Thévenot, K. Toth, R.A. Durst, G.S. Wilson, Electrochemical biosensors: recommended definitions and classification1International Union of Pure and Applied Chemistry: Physical Chemistry Division, Commission I.7 (Biophysical Chemistry); Analytical Chemistry Division, Commission V.5 (Electroanalytical Chemistry).1, Biosens. Bioelectron. 16 (2001) 121–131. https://doi.org/10.1016/S0956-5663(01)00115-4.

[12] A. Hulanicki, S. Glab, F. Ingman, Chemical sensors: definitions and classification, Pure Appl. Chem. 63 (1991) 1247–1250. https://doi.org/10.1351/pac199163091247.

[13] S.I. Kaya, G. Ozcelikay, F. Mollarasouli, N.K. Bakirhan, S.A. Ozkan, Recent achievements and challenges on nanomaterial based electrochemical biosensors for the detection of colon and lung cancer biomarkers, Sens. Actuators B Chem. 351 (2022) 130856. https://doi.org/10.1016/j.snb.2021.130856.

[14] Varnakavi. Naresh, N. Lee, A Review on Biosensors and Recent Development of Nanostructured Materials-Enabled Biosensors, Sensors. 21 (2021) 1109. https://doi.org/10.3390/s21041109.

[15] A.A. Hamzah, Sh. Nadzirah, Biosensor Development, in: Encycl. Sens. Biosens., Elsevier, 2023: pp. 209–217. https://linkinghub.elsevier.com/retrieve/pii/B9780128225486001126 (accessed February 22, 2023).

[16] A. Pereira, M. Sales, L. Rodrigues, Biosensors for Rapid Detection of Breast Cancer Biomarkers, in: Adv. Biosens. Health Care Appl., Elsevier, 2019: pp. 71–103. https://doi.org/10.1016/B978-0-12-815743-5.00003-2.

[17] C. Direksilp, N. Parinyanitikul, N. Ariyasajjamongkol, A. Sirivat, A label-free electrochemical immunosensor based on 11-mercaptoundecanoic acid grafted chitosan and poly(N-methylaniline) for the detection of carcinoembryonic antigen, Bioelectrochemistry. 152 (2023) 108446. https://doi.org/10.1016/j.bioelechem.2023.108446.

[18] S. Wignarajah, I. Chianella, I.E. Tothill, Development of Electrochemical Immunosensors for HER-1 and HER-2 Analysis in Serum for Breast Cancer Patients, Biosensors. 13 (2023) 355. https://doi.org/10.3390/bios13030355.

[19] Y. Yue, X. Chen, J. Wang, M. Ma, A. He, R. Liu, Label-free electrochemical biosensor with magnetically induced self-assembly for the detection of cancer antigen 125, Arab. J. Chem. 16 (2023) 105070. https://doi.org/10.1016/j.arabjc.2023.105070.

[20] Z. Shekari, H.R. Zare, A. Falahati, Electrochemical sandwich aptasensor for the carcinoembryonic antigen using graphene quantum dots, gold nanoparticles and nitrogen doped graphene modified electrode and exploiting the peroxidase-mimicking activity of a G-quadruplex DNAzyme, Microchim. Acta. 186 (2019) 530. https://doi.org/10.1007/s00604-019-3572-9.

[21] F. Ben Moussa, Molecularly imprinted polymers meet electrochemical cancer chemosensors: A critical review from a clinical and economic perspective, Microchem. J. 191 (2023) 108838. https://doi.org/10.1016/j.microc.2023.108838.

[22] T.A. Tabish, H. Hayat, A. Abbas, R.J. Narayan, Graphene quantum dot–based electrochemical biosensing for early cancer detection, Curr. Opin. Electrochem. 30 (2021) 100786. https://doi.org/10.1016/j.coelec.2021.100786.

[23] S. Li, Q. Ma, Electrochemical nano-sensing interface for exosomes analysis and cancer diagnosis, Biosens. Bioelectron. 214 (2022) 114554. https://doi.org/10.1016/j.bios.2022.114554.

[24] J. Kappen, M. Skorupa, K. Krukiewicz, Conducting Polymers as Versatile Tools for the Electrochemical Detection of Cancer Biomarkers, Biosensors. 13 (2022) 31. https://doi.org/10.3390/bios13010031.

[25] I.M. Mostafa, Y. Tian, S. Anjum, S. Hanif, M. Hosseini, B. Lou, G. Xu, Comprehensive review on the electrochemical biosensors of different breast cancer biomarkers, Sens. Actuators B Chem. 365 (2022) 131944. https://doi.org/10.1016/j.snb.2022.131944.

[26] T. Pozzo, S.M. Higdon, S. Pattathil, M.G. Hahn, A.B. Bennett, Characterization of novel glycosyl hydrolases discovered by cell wall glycan directed monoclonal antibody screening and metagenome analysis of maize aerial root mucilage, PLOS ONE. 13 (2018) e0204525. https://doi.org/10.1371/journal.pone.0204525.

[27] M. Siddiqui, Monoclonal antibodies as diagnostics; an appraisal, Indian J. Pharm. Sci. 72 (2010) 12. https://doi.org/10.4103/0250-474X.62229.

[28] F. Ricci, G. Adornetto, G. Palleschi, A review of experimental aspects of electrochemical immunosensors, Electrochimica Acta. 84 (2012) 74–83. https://doi.org/10.1016/j.electacta.2012.06.033.

[29] H.F. Stills, Polyclonal Antibody Production, in: Lab. Rabbit Guin. Pig Hamst. Rodents, Elsevier, 2012: pp. 259–274. https://doi.org/10.1016/B978-0-12-380920-9.00011-0.

[30] F. Li, N. Vijayasankaran, A. (Yijuan) Shen, R. Kiss, A. Amanullah, Cell culture processes for monoclonal antibody production, MAbs. 2 (2010) 466–479. https://doi.org/10.4161/mabs.2.5.12720.

[31] K. Usui-Aoki, K. Shimada, H. Koga, A novel antibody microarray format using non-covalent antibody immobilization with chemiluminescent detection, Mol BioSyst. 3 (2007) 36–42. https://doi.org/10.1039/B612492E.

[32] J. Liu, J. Wang, T. Wang, D. Li, F. Xi, J. Wang, E. Wang, Three-dimensional electrochemical immunosensor for sensitive detection of carcinoembryonic antigen based on monolithic and macroporous graphene foam, Biosens. Bioelectron. 65 (2015) 281–286. https://doi.org/10.1016/j.bios.2014.10.016.

[33] E. von Witting, S. Hober, S. Kanje, Affinity-Based Methods for Site-Specific Conjugation of Antibodies, Bioconjug. Chem. 32 (2021) 1515–1524. https://doi.org/10.1021/acs.bioconjchem.1c00313.

[34] M. Vestergaard, K. Kerman, E. Tamiya, An Overview of Label-free Electrochemical Protein Sensors, Sensors. 7 (2007) 3442–3458. https://doi.org/10.3390/s7123442.

[35] X. Li, L. Liu, Z. Xu, W. Wang, J. Shi, L. Liu, M. Jing, F. Li, X. Zhang, Gamma irradiation and microemulsion assisted synthesis of monodisperse flower-like platinum-gold nanoparticles/reduced graphene oxide nanocomposites for ultrasensitive detection of carcinoembryonic antigen, Sens. Actuators B Chem. 287 (2019) 267–277. https://doi.org/10.1016/j.snb.2019.02.026.

[36] J. Wang, N. Hui, Zwitterionic poly(carboxybetaine) functionalized conducting polymer polyaniline nanowires for the electrochemical detection of carcinoembryonic antigen in undiluted blood serum, Bioelectrochemistry. 125 (2019) 90–96. https://doi.org/10.1016/j.bioelechem.2018.09.006.

[37] F. Khosravi, M. Rahaie, M.R. Ghaani, M. Azimzadeh, E. Mostafavi, Ultrasensitive electrochemical miR-155 nanocomposite biosensor based on functionalized/conjugated graphene materials and gold nanostars, Sens. Actuators B Chem. 375 (2023) 132877. https://doi.org/10.1016/j.snb.2022.132877.

[38] X. Cai, S. Weng, R. Guo, L. Lin, W. Chen, Z. Zheng, Z. Huang, X. Lin, Ratiometric electrochemical immunoassay based on internal reference value for reproducible and sensitive detection of tumor marker, Biosens. Bioelectron. 81 (2016) 173–180. https://doi.org/10.1016/j.bios.2016.02.066.

[39] P. Butmee, G. Tumcharern, G. Thouand, K. Kalcher, A. Samphao, An ultrasensitive immunosensor based on manganese dioxide-graphene nanoplatelets and core shell Fe3O4@Au nanoparticles for label-free detection of carcinoembryonic antigen, Bioelectrochemistry. 132 (2020) 107452. https://doi.org/10.1016/j.bioelechem.2019.107452.

[40] S. Biswas, Q. Lan, C. Li, X.-H. Xia, Morphologically Flex Sm-MOF Based Electrochemical Immunosensor for Ultrasensitive Detection of a Colon Cancer Biomarker, Anal. Chem. 94 (2022) 3013–3019. https://doi.org/10.1021/acs.analchem.1c05538.

[41] A.C.H. de Castro, L.M. Alves, A.C.S. Siquieroli, J.M. Madurro, A.G. Brito-Madurro, Label-free electrochemical immunosensor for detection of oncomarker CA125 in serum, Microchem. J. 155 (2020) 104746. https://doi.org/10.1016/j.microc.2020.104746.

[42] Y. Fan, S. Shi, J. Ma, Y. Guo, Smartphone-based electrochemical system with multi-walled carbon nanotubes/thionine/gold nanoparticles modified screen-printed immunosensor for cancer antigen 125 detection, Microchem. J. 174 (2022) 107044. https://doi.org/10.1016/j.microc.2021.107044.

[43] Z. Huang, Z. Jiang, C. Zhao, W. Han, L. Lin, A. Liu, S. Weng, X. Lin, Simple and effective label-free electrochemical immunoassay for carbohydrate antigen 19-9 based on polythionine-Au composites as enhanced sensing signals for detecting different clinical samples, Int. J. Nanomedicine. Volume 12 (2017) 3049–3058. https://doi.org/10.2147/IJN.S131805.

[44] P. Ranjan, M. Abubakar Sadique, S. Yadav, R. Khan, An Electrochemical Immunosensor Based on Gold-Graphene Oxide Nanocomposites with Ionic Liquid for Detecting the Breast Cancer CD44 Biomarker, ACS Appl. Mater. Interfaces. 14 (2022) 20802–20812. https://doi.org/10.1021/acsami.2c03905.

[45] S. Kongkaew, S. Cotchim, P. Kanatharana, P. Thavarungkul, W. Limbut, Disposable label-free electrochemical immunosensor based on prussian blue nanocubes for four breast cancer tumor markers, Talanta. 255 (2023) 124229. https://doi.org/10.1016/j.talanta.2022.124229.

[46] P. Ranjan, S. Yadav, M.A. Sadique, R. Khan, A.K. Srivastava, Ionic Liquid-Functionalized ZrO_2 /Reduced Graphene Oxide Nanocomposites for Carcinoembryonic Antigen Electrochemical Detection, ACS Appl. Nano Mater. 5 (2022) 14999–15010. https://doi.org/10.1021/acsanm.2c03212.

[47] R. Zhang, C. Rejeeth, W. Xu, C. Zhu, X. Liu, J. Wan, M. Jiang, K. Qian, Label-Free Electrochemical Sensor for CD44 by Ligand-Protein Interaction, Anal. Chem. 91 (2019) 7078–7085. https://doi.org/10.1021/acs.analchem.8b05966.

[48] P. Gulati, P. Mishra, M. Khanuja, J. Narang, S.S. Islam, Nano-moles detection of tumor specific biomarker DNA for colorectal cancer detection using vertically aligned multi-wall carbon nanotubes based flexible electrodes, Process Biochem. 90 (2020) 184–192. https://doi.org/10.1016/j.procbio.2019.11.021.

[49] J. Wang, D. Wang, N. Hui, A low fouling electrochemical biosensor based on the zwitterionic polypeptide doped conducting polymer PEDOT for breast cancer marker BRCA1 detection, Bioelectrochemistry. 136 (2020) 107595. https://doi.org/10.1016/j.bioelechem.2020.107595.

[50] Y. Xia, M. Li, C. Chen, M. Xia, W. Zhang, W. Gao, Employing Label-free Electrochemical Biosensor Based on 3D-Reduced Graphene Oxide and Polyaniline Nanofibers for Ultrasensitive Detection of Breast Cancer BRCA1 Biomarker, Electroanalysis. 32 (2020) 2045–2055. https://doi.org/10.1002/elan.202060039.

[51] S.C. Barman, M.F. Hossain, H. Yoon, J.Y. Park, Trimetallic Pd@Au@Pt nanocomposites platform on -COOH terminated reduced graphene oxide for highly sensitive CEA and PSA biomarkers detection, Biosens. Bioelectron. 100 (2018) 16–22. https://doi.org/10.1016/j.bios.2017.08.045.

[52] C. Pothipor, S. Bamrungsap, J. Jakmunee, K. Ounnunkad, A gold nanoparticle-dye/poly(3-aminobenzylamine)/two dimensional MoSe2/graphene oxide electrode towards label-free electrochemical biosensor for simultaneous dual-mode detection of cancer antigen 15-3 and microRNA-21, Colloids Surf. B Biointerfaces. 210 (2022) 112260. https://doi.org/10.1016/j.colsurfb.2021.112260.

[53] X. Pei, B. Zhang, J. Tang, B. Liu, W. Lai, D. Tang, Sandwich-type immunosensors and immunoassays exploiting nanostructure labels: A review, Anal. Chim. Acta. 758 (2013) 1–18. https://doi.org/10.1016/j.aca.2012.10.060.

[54] I.-H. Cho, J. Lee, J. Kim, M. Kang, J. Paik, S. Ku, H.-M. Cho, J. Irudayaraj, D.-H. Kim, Current Technologies of Electrochemical Immunosensors: Perspective on Signal Amplification, Sensors. 18 (2018) 207. https://doi.org/10.3390/s18010207.

[55] H. Filik, A.A. Avan, Nanostructures for nonlabeled and labeled electrochemical immunosensors: Simultaneous electrochemical detection of cancer markers: A review, Talanta. 205 (2019) 120153. https://doi.org/10.1016/j.talanta.2019.120153.

[56] E. Mostafavi, S. Iravani, MXene-Graphene Composites: A Perspective on Biomedical Potentials, Nano-Micro Lett. 14 (2022) 130. https://doi.org/10.1007/s40820-022-00880-y.

[57] S. Akbari Nakhjavani, H. Afsharan, B. Khalilzadeh, M.H. Ghahremani, S. Carrara, Y. Omidi, Gold and silver bio/nano-hybrids-based electrochemical immunosensor for ultrasensitive detection of carcinoembryonic antigen, Biosens. Bioelectron. 141 (2019) 111439. https://doi.org/10.1016/j.bios.2019.111439.

[58] C. Ma, C. Zhao, W. Li, Y. Song, C. Hong, X. Qiao, Sandwich-type electrochemical immunosensor constructed using three-dimensional lamellar stacked CoS2@C hollow nanotubes prepared by template-free method to detect carcinoembryonic antigen, Anal. Chim. Acta. 1088 (2019) 54–62. https://doi.org/10.1016/j.aca.2019.09.007.

[59] S. Su, Q. Sun, L. Wan, X. Gu, D. Zhu, Y. Zhou, J. Chao, L. Wang, Ultrasensitive analysis of carcinoembryonic antigen based on MoS2-based electrochemical immunosensor with triple signal amplification, Biosens. Bioelectron. 140 (2019) 111353. https://doi.org/10.1016/j.bios.2019.111353.

[60] Z. Tan, L. Cao, Y. Yang, Q. Yan, Q. Liu, W. Zhang, P. Zhao, Y. Li, D. Zhang, Amperometric immunoassay for the carcinoembryonic antigen by using a peroxidase mimic consisting of palladium nanospheres functionalized with glutathione-capped gold nanoparticles on graphene oxide, Microchim. Acta. 186 (2019) 693. https://doi.org/10.1007/s00604-019-3799-5.

[61] C. Zhao, C. Ma, M. Wu, W. Li, Y. Song, Y. Yang, B. Yin, C. Hong, X. Qiao, An immunosensor detects carcinoembryonic antigen by a double reduction strategy based on polyphenylamine as a sacrifice reducing agent, Int. J. Hydrog. Energy. 45 (2020) 5055–5066. https://doi.org/10.1016/j.ijhydene.2019.12.041.

[62] E. Ma, P. Wang, Q. Yang, H. Yu, F. Pei, Y. Li, Q. Liu, Y. Dong, Electrochemical immunosensor based on MoS2 NFs/Au@AgPt YNCs as signal amplification label for sensitive detection of CEA, Biosens. Bioelectron. 142 (2019) 111580. https://doi.org/10.1016/j.bios.2019.111580.

[63] W. Li, X. Qiao, C. Hong, C. Ma, Y. Song, A sandwich-type electrochemical immunosensor for detecting CEA based on CeO2-MoS2 absorbed Pb2+, Anal. Biochem. 592 (2020) 113566. https://doi.org/10.1016/j.ab.2019.113566.

[64] Y. Chen, A.-J. Wang, P.-X. Yuan, X. Luo, Y. Xue, J.-J. Feng, Three dimensional sea-urchin-like PdAuCu nanocrystals/ferrocene-grafted-polylysine as an efficient probe to amplify the electrochemical signals for ultrasensitive immunoassay of carcinoembryonic antigen, Biosens. Bioelectron. 132 (2019) 294–301. https://doi.org/10.1016/j.bios.2019.02.057.

[65] X. Gu, Z. She, T. Ma, S. Tian, H.-B. Kraatz, Electrochemical detection of carcinoembryonic antigen, Biosens. Bioelectron. 102 (2018) 610–616. https://doi.org/10.1016/j.bios.2017.12.014.

[66] Y. Chen, Y. Li, D. Deng, H. He, X. Yan, Z. Wang, C. Fan, L. Luo, Effective immobilization of Au nanoparticles on TiO2 loaded graphene for a novel sandwich-type immunosensor, Biosens. Bioelectron. 102 (2018) 301–306. https://doi.org/10.1016/j.bios.2017.11.009.

[67] C. Pothipor, N. Wiriyakun, T. Putnin, A. Ngamaroonchote, J. Jakmunee, K. Ounnunkad, R. Laocharoensuk, N. Aroonyadet, Highly sensitive biosensor based on graphene–poly (3-aminobenzoic acid) modified electrodes and porous-hollowed-silver-gold nanoparticle labelling for prostate cancer detection, Sens. Actuators B Chem. 296 (2019) 126657. https://doi.org/10.1016/j.snb.2019.126657.

[68] H. Ehzari, M. Amiri, M. Safari, Enzyme-free sandwich-type electrochemical immunosensor for highly sensitive prostate specific antigen based on conjugation of quantum dots and antibody on surface of modified glassy carbon electrode with core–shell magnetic metal-organic frameworks, Talanta. 210 (2020) 120641. https://doi.org/10.1016/j.talanta.2019.120641.

[69] Y. Wang, G. Zhao, H. Wang, W. Cao, B. Du, Q. Wei, Sandwich-type electrochemical immunoassay based on Co3O4@MnO2-thionine and pseudo-ELISA method toward sensitive detection of alpha fetoprotein, Biosens. Bioelectron. 106 (2018) 179–185. https://doi.org/10.1016/j.bios.2018.02.002.

[70] D. Sun, H. Li, M. Li, C. Li, L. Qian, B. Yang, Electrochemical immunosensors with AuPt-vertical graphene/glassy carbon electrode for alpha-fetoprotein detection based on label-free and sandwich-type strategies, Biosens. Bioelectron. 132 (2019) 68–75. https://doi.org/10.1016/j.bios.2019.02.045.

[71] F.-M. Wang, S.-H. Huang, C.-C. Yuan, C.-T. Yeh, W.-L. Chen, X.-C. Wang, N. Runprapan, Y.-J. Tsai, Y.-L. Chuang, C.-H. Su, Detection of O-glycosylated CA125 by using an electrochemical immunosensor for ovarian cancer diagnosis, J. Appl. Electrochem. 50 (2020) 1189–1198. https://doi.org/10.1007/s10800-020-01477-2.

[72] D. Kalyoncu, Y.T. Buyuksunetci, Ü. Anık, Development of a Sandwich Immunosensor for concurrent detection of carcinoembryonic antigen (CEA), vascular endothelial growth factor (VEGF) and α-fetoprotein (AFP) biomarkers, Mater. Sci. Eng. C. 101 (2019) 88–91. https://doi.org/10.1016/j.msec.2019.03.079.

[73] L. Yu, X. Cui, H. Li, J. Lu, Q. Kang, D. Shen, A ratiometric electrochemical sensor for multiplex detection of cancer biomarkers using bismuth as an internal reference and metal sulfide nanoparticles as signal tags, The Analyst. 144 (2019) 4073–4080. https://doi.org/10.1039/C9AN00775J.

[74] N. Wang, X. Zhao, H. Chen, L. Bai, H. Xu, W. Wang, H. Yang, D. Wei, L. Yang, Fabrication of novel electrochemical immunosensor by mussel-inspired chemistry and surface-initiated PET-ATRP for the simultaneous detection of CEA and AFP, React. Funct. Polym. 154 (2020) 104632. https://doi.org/10.1016/j.reactfunctpolym.2020.104632.

[75] W. Li, Y. Yang, C. Ma, Y. Song, X. Qiao, C. Hong, A sandwich-type electrochemical immunosensor for ultrasensitive detection of multiple tumor markers using an electrical signal difference strategy, Talanta. 219 (2020) 121322. https://doi.org/10.1016/j.talanta.2020.121322.

[76] A.D. Ellington, J.W. Szostak, In vitro selection of RNA molecules that bind specific ligands, Nature. 346 (1990) 818–822. https://doi.org/10.1038/346818a0.

[77] L. Gold, SELEX: How It Happened and Where It will Go, J. Mol. Evol. 81 (2015) 140–143. https://doi.org/10.1007/s00239-015-9705-9.

[78] A.D. Ellington, J.W. Szostak, Selection in vitro of single-stranded DNA molecules that fold into specific ligand-binding structures, Nature. 355 (1992) 850–852. https://doi.org/10.1038/355850a0.

[79] Y.X. Wu, Y.J. Kwon, Aptamers: The "evolution" of SELEX, Methods. 106 (2016) 21–28. https://doi.org/10.1016/j.ymeth.2016.04.020.

[80] A. Díaz-Fernández, R. Lorenzo-Gómez, R. Miranda-Castro, N. de-los-Santos-Álvarez, M.J. Lobo-Castañón, Electrochemical aptasensors for cancer diagnosis in biological fluids – A review, Anal. Chim. Acta. 1124 (2020) 1–19. https://doi.org/10.1016/j.aca.2020.04.022.

[81] K. Malecka, E. Mikuła, E.E. Ferapontova, Design Strategies for Electrochemical Aptasensors for Cancer Diagnostic Devices, Sensors. 21 (2021) 736. https://doi.org/10.3390/s21030736.

[82] A. Rhouati, G. Catanante, G. Nunes, A. Hayat, J.-L. Marty, Label-Free Aptasensors for the Detection of Mycotoxins, Sensors. 16 (2016) 2178. https://doi.org/10.3390/s16122178.

[83] J. Liu, M.D. Morris, F.C. Macazo, L.R. Schoukroun-Barnes, R.J. White, The Current and Future Role of Aptamers in Electroanalysis, J. Electrochem. Soc. 161 (2014) H301–H313. https://doi.org/10.1149/2.026405jes.

[84] K. Malecka, E. Mikuła, E.E. Ferapontova, Design Strategies for Electrochemical Aptasensors for Cancer Diagnostic Devices, Sensors. 21 (2021) 736. https://doi.org/10.3390/s21030736.

[85] P. Jolly, P. Zhurauski, J.L. Hammond, A. Miodek, S. Liébana, T. Bertok, J. Tkáč, P. Estrela, Self-assembled gold nanoparticles for impedimetric and amperometric detection of a prostate cancer biomarker, Sens. Actuators B Chem. 251 (2017) 637–643. https://doi.org/10.1016/j.snb.2017.05.040.

[86] A. Raouafi, A. Sánchez, N. Raouafi, R. Villalonga, Electrochemical aptamer-based bioplatform for ultrasensitive detection of prostate specific antigen, Sens. Actuators B Chem. 297 (2019) 126762. https://doi.org/10.1016/j.snb.2019.126762.

[87] B. Zhang, H. Ding, Q. Chen, T. Wang, K. Zhang, Prussian blue nanoparticle-labeled aptasensing platform on graphene oxide for voltammetric detection of α-fetoprotein in hepatocellular carcinoma with target recycling, The Analyst. 144 (2019) 4858–4864. https://doi.org/10.1039/C9AN01029G.

[88] P.F. Rostamabadi, E. Heydari-Bafrooei, Impedimetric aptasensing of the breast cancer biomarker HER2 using a glassy carbon electrode modified with gold nanoparticles in a composite consisting of electrochemically reduced graphene oxide and single-walled carbon nanotubes, Microchim. Acta. 186 (2019) 495. https://doi.org/10.1007/s00604-019-3619-y.

[89] F. Zhang, L. Fan, Z. Liu, Y. Han, Y. Guo, A label-free electrochemical aptasensor for the detection of cancer antigen 125 based on nickel hexacyanoferrate nanocubes/polydopamine functionalized graphene, J. Electroanal. Chem. 918 (2022) 116424. https://doi.org/10.1016/j.jelechem.2022.116424.

[90] Y. Zhang, N. Li, Y. Xu, M. Yang, X. Luo, C. Hou, D. Huo, An ultra-sensitive electrochemical aptasensor based on Co-MOF/ZIF-8 nano-thin-film by the in-situ electrochemical synthesis for simultaneous detection of multiple biomarkers of breast cancer, Microchem. J. 187 (2023) 108316. https://doi.org/10.1016/j.microc.2022.108316.

[91] Y. Zhang, N. Li, Y. Xu, X. Liu, Y. Ma, Z. Huang, H. Luo, C. Hou, D. Huo, A novel electrochemical biosensor based on AMNFs@ZIF-67 nano composite material for ultrasensitive detection of HER2, Bioelectrochemistry. 150 (2023) 108362. https://doi.org/10.1016/j.bioelechem.2022.108362.

[92] S. Forouzanfar, F. Alam, N. Pala, C. Wang, Highly sensitive label-free electrochemical aptasensors based on photoresist derived carbon for cancer biomarker detection, Biosens. Bioelectron. 170 (2020) 112598. https://doi.org/10.1016/j.bios.2020.112598.

[93] H.B. Seo, M.B. Gu, Aptamer-based sandwich-type biosensors, J. Biol. Eng. 11 (2017) 11. https://doi.org/10.1186/s13036-017-0054-7.

[94] L. Xu, Z. Liu, S. Lei, D. Huang, L. Zou, B. Ye, A sandwich-type electrochemical aptasensor for the carcinoembryonic antigen via biocatalytic precipitation amplification and by using gold nanoparticle composites, Microchim. Acta. 186 (2019) 473. https://doi.org/10.1007/s00604-019-3542-2.

[95] M. Sadasivam, A. Sakthivel, N. Nagesh, S. Hansda, M. Veerapandian, S. Alwarappan, P. Manickam, Magnetic bead-amplified voltammetric detection for carbohydrate antigen 125 with enzyme labels using aptamer-antigen-antibody sandwiched assay, Sens. Actuators B Chem. 312 (2020) 127985. https://doi.org/10.1016/j.snb.2020.127985.

[96] M. Jarczewska, A. Trojan, M. Gągała, E. Malinowska, Studies on the Affinity-based Biosensors for Electrochemical Detection of HER2 Cancer Biomarker, Electroanalysis. 31 (2019) 1125–1134. https://doi.org/10.1002/elan.201900041.

[97] M. Jarczewska, J. Wieczorek, E. Malinowska, Electrochemical Studies on the Binding of Antibody—Aptamer Hybrid Receptor Layers to HER2 Protein, J. Electrochem. Soc. 167 (2020) 067512. https://doi.org/10.1149/1945-7111/ab80ac.

[98] P. Yang, X. Li, L. Wang, Q. Wu, Z. Chen, X. Lin, Sandwich-type amperometric immunosensor for cancer biomarker based on signal amplification strategy of multiple enzyme-linked antibodies as probes modified with carbon nanotubes and concanavalin A, J. Electroanal. Chem. 732 (2014) 38–45. https://doi.org/10.1016/j.jelechem.2014.08.030.

[99] Y. Wu, P. Xue, Y. Kang, K.M. Hui, Highly Specific and Ultrasensitive Graphene-Enhanced Electrochemical Detection of Low-Abundance Tumor Cells Using Silica Nanoparticles Coated with Antibody-Conjugated Quantum Dots, Anal. Chem. 85 (2013) 3166–3173. https://doi.org/10.1021/ac303398b.

[100] Y. Wang, S. Sun, J. Luo, Y. Xiong, T. Ming, J. Liu, Y. Ma, S. Yan, Y. Yang, Z. Yang, J. Reboud, H. Yin, J.M. Cooper, X. Cai, Low sample volume origami-paper-based graphene-modified aptasensors for label-free electrochemical detection of cancer biomarker-EGFR, Microsyst. Nanoeng. 6 (2020) 32. https://doi.org/10.1038/s41378-020-0146-2.

[101] S. Forouzanfar, F. Alam, N. Pala, C. Wang, Review—A Review of Electrochemical Aptasensors for Label-Free Cancer Diagnosis, J. Electrochem. Soc. 167 (2020) 067511. https://doi.org/10.1149/1945-7111/ab7f20.

[102] P. Rebelo, E. Costa-Rama, I. Seguro, J.G. Pacheco, H.P.A. Nouws, M.N.D.S. Cordeiro, C. Delerue-Matos, Molecularly imprinted polymer-based electrochemical sensors for environmental analysis, Biosens. Bioelectron. 172 (2021) 112719. https://doi.org/10.1016/j.bios.2020.112719.

[103] F.H. Dickey, The Preparation of Specific Adsorbents, Proc. Natl. Acad. Sci. 35 (1949) 227–229. https://doi.org/10.1073/pnas.35.5.227.

[104] M.A. Beluomini, J.L. da Silva, A.C. de Sá, E. Buffon, T.C. Pereira, N.R. Stradiotto, Electrochemical sensors based on molecularly imprinted polymer on nanostructured carbon materials: A review, J. Electroanal. Chem. 840 (2019) 343–366. https://doi.org/10.1016/j.jelechem.2019.04.005.

[105] R.D. Crapnell, N.C. Dempsey-Hibbert, M. Peeters, A. Tridente, C.E. Banks, Molecularly imprinted polymer based electrochemical biosensors: Overcoming the challenges of detecting vital biomarkers and speeding up diagnosis, Talanta Open. 2 (2020) 100018. https://doi.org/10.1016/j.talo.2020.100018.

[106] S. Ramanavicius, A. Ramanavicius, Development of molecularly imprinted polymer based phase boundaries for sensors design (review), Adv. Colloid Interface Sci. 305 (2022) 102693. https://doi.org/10.1016/j.cis.2022.102693.

[107] K.K. Dar, S. Shao, T. Tan, Y. Lv, Molecularly imprinted polymers for the selective recognition of microorganisms, Biotechnol. Adv. 45 (2020) 107640. https://doi.org/10.1016/j.biotechadv.2020.107640.

[108] S. Basak, R. Venkatram, R.S. Singhal, Recent advances in the application of molecularly imprinted polymers (MIPs) in food analysis, Food Control. 139 (2022) 109074. https://doi.org/10.1016/j.foodcont.2022.109074.

[109] A.A. Lahcen, A. Amine, Recent Advances in Electrochemical Sensors Based on Molecularly Imprinted Polymers and Nanomaterials, Electroanalysis. 31 (2019) 188–201. https://doi.org/10.1002/elan.201800623.

[110] J. Kalecki, Z. Iskierko, M. Cieplak, P.S. Sharma, Oriented Immobilization of Protein Templates: A New Trend in Surface Imprinting, ACS Sens. 5 (2020) 3710–3720. https://doi.org/10.1021/acssensors.0c01634.

[111] Z. Yazdani, H. Yadegari, H. Heli, A molecularly imprinted electrochemical nanobiosensor for prostate specific antigen determination, Anal. Biochem. 566 (2019) 116–125. https://doi.org/10.1016/j.ab.2018.11.020.

[112] Y. Ma, X.-L. Shen, Q. Zeng, L.-S. Wang, A glassy carbon electrode modified with graphene nanoplatelets, gold nanoparticles and chitosan, and coated with a molecularly imprinted polymer for highly sensitive determination of prostate specific antigen, Microchim. Acta. 184 (2017) 4469–4476. https://doi.org/10.1007/s00604-017-2458-y.

[113] L. Abbasy, A. Mohammadzadeh, M. Hasanzadeh, N. Razmi, Development of a reliable bioanalytical method based on prostate specific antigen trapping on the cavity of molecular imprinted polymer towards sensing of

PSA using binding affinity of PSA-MIP receptor: A novel biosensor, J. Pharm. Biomed. Anal. 188 (2020) 113447. https://doi.org/10.1016/j.jpba.2020.113447.

[114] Y. Lai, C. Zhang, Y. Deng, G. Yang, S. Li, C. Tang, N. He, A novel α-fetoprotein-MIP immunosensor based on AuNPs/PTh modified glass carbon electrode, Chin. Chem. Lett. 30 (2019) 160–162. https://doi.org/10.1016/j.cclet.2018.07.011.

[115] J.G. Pacheco, M.S.V. Silva, M. Freitas, H.P.A. Nouws, C. Delerue-Matos, Molecularly imprinted electrochemical sensor for the point-of-care detection of a breast cancer biomarker (CA 15-3), Sens. Actuators B Chem. 256 (2018) 905–912. https://doi.org/10.1016/j.snb.2017.10.027.

[116] J.A. Ribeiro, C.M. Pereira, A.F. Silva, M.G.F. Sales, Disposable electrochemical detection of breast cancer tumour marker CA 15-3 using poly(Toluidine Blue) as imprinted polymer receptor, Biosens. Bioelectron. 109 (2018) 246–254. https://doi.org/10.1016/j.bios.2018.03.011.

[117] R.S. Gomes, F.T.C. Moreira, R. Fernandes, M.G.F. Sales, Sensing CA 15-3 in point-of-care by electropolymerizing O-phenylenediamine (oPDA) on Au-screen printed electrodes, PLOS ONE. 13 (2018) e0196656. https://doi.org/10.1371/journal.pone.0196656.

[118] A. Santos, F. Moreira, L. Helguero, M. Sales, Antibody Biomimetic Material Made of Pyrrole for CA 15-3 and Its Application as Sensing Material in Ion-Selective Electrodes for Potentiometric Detection, Biosensors. 8 (2018) 8. https://doi.org/10.3390/bios8010008.

[119] F.T.C. Moreira, M.J.M.S. Ferreira, J.R.T. Puga, M.G.F. Sales, Screen-printed electrode produced by printed-circuit board technology. Application to cancer biomarker detection by means of plastic antibody as sensing material, Sens. Actuators B Chem. 223 (2016) 927–935. https://doi.org/10.1016/j.snb.2015.09.157.

[120] X. Shen, Y. Ma, Q. Zeng, J. Huang, J. Tao, L. Wang, Ultrasensitive Determination of Human Chorionic Gonadotropin using a Molecularly Imprinted Electrochemical Sensor, ChemistrySelect. 2 (2017) 6549–6555. https://doi.org/10.1002/slct.201700962.

[121] T.S.C.R. Rebelo, R. Costa, A.T.S.C. Brandão, A.F. Silva, M.G.F. Sales, C.M. Pereira, Molecularly imprinted polymer SPE sensor for analysis of CA-125 on serum, Anal. Chim. Acta. 1082 (2019) 126–135. https://doi.org/10.1016/j.aca.2019.07.050.

[122] B. Bozal-Palabiyik, M. Lettieri, B. Uslu, G. Marrazza, Electrochemical Detection of Vascular Endothelial Growth Factor by Molecularly Imprinted Polymer, Electroanalysis. 31 (2019) 1458–1464. https://doi.org/10.1002/elan.201900185.

[123] T. Alizadeh, S. Nayeri, An enzyme-free sensing platform based on molecularly imprinted polymer/MWCNT composite for sub-micromolar-level determination of pyruvic acid as a cancer biomarker, Anal. Bioanal. Chem. 412 (2020) 657–667. https://doi.org/10.1007/s00216-019-02273-4.

[124] F. Ben Moussa, F. Achi, H. Meskher, A. Henni, H. Belkhalfa, Green one-step reduction approach to prepare rGO@AgNPs coupled with molecularly imprinted polymer for selective electrochemical detection of lactic acid as a cancer biomarker, Mater. Chem. Phys. 289 (2022) 126456. https://doi.org/10.1016/j.matchemphys.2022.126456.

[125] J.G. Pacheco, P. Rebelo, M. Freitas, H.P.A. Nouws, C. Delerue-Matos, Breast cancer biomarker (HER2-ECD) detection using a molecularly imprinted electrochemical sensor, Sens. Actuators B Chem. 273 (2018) 1008–1014. https://doi.org/10.1016/j.snb.2018.06.113.

[126] Y. Lai, Y. Deng, G. Yang, S. Li, C. Zhang, X. Liu, Molecular Imprinting Polymers Electrochemical Sensor Based on AuNPs/PTh Modified GCE for Highly Sensitive Detection of Carcinomaembryonic Antigen, J. Biomed. Nanotechnol. 14 (2018) 1688–1694. https://doi.org/10.1166/jbn.2018.2617.

[127] J. Liu, Y. Wang, X. Liu, Q. Yuan, Y. Zhang, Y. Li, Novel molecularly imprinted polymer (MIP) multiple sensors for endogenous redox couples determination and their applications in lung cancer diagnosis, Talanta. 199 (2019) 573–580. https://doi.org/10.1016/j.talanta.2019.03.018.

[128] P. Karami, H. Bagheri, M. Johari-Ahar, H. Khoshsafar, F. Arduini, A. Afkhami, Dual-modality impedimetric immunosensor for early detection of prostate-specific antigen and myoglobin markers based on antibody-molecularly imprinted polymer, Talanta. 202 (2019) 111–122. https://doi.org/10.1016/j.talanta.2019.04.061.

[129] T.P. Nguy, T. Van Phi, D.T.N. Tram, K. Eersels, P. Wagner, T.T.N. Lien, Development of an impedimetric sensor for the label-free detection of the amino acid sarcosine with molecularly imprinted polymer receptors, Sens. Actuators B Chem. 246 (2017) 461–470. https://doi.org/10.1016/j.snb.2017.02.101.

[130] M. Johari-Ahar, P. Karami, M. Ghanei, A. Afkhami, H. Bagheri, Development of a molecularly imprinted polymer tailored on disposable screen-printed electrodes for dual detection of EGFR and VEGF using nano-liposomal amplification strategy, Biosens. Bioelectron. 107 (2018) 26–33. https://doi.org/10.1016/j.bios.2018.02.005.

[131] X. Ma, A strategy for construction of highly sensitive glycosyl imprinted electrochemical sensor based on sandwich-like multiple signal enhancement and determination of neural cell adhesion molecule, Biosens. Bioelectron. (2020) 7.

[132] M.-H. Lee, J.L. Thomas, Y.-C. Chang, Y.-S. Tsai, B.-D. Liu, H.-Y. Lin, Electrochemical sensing of nuclear matrix protein 22 in urine with molecularly imprinted poly(ethylene-co-vinyl alcohol) coated zinc oxide nanorod arrays for clinical studies of bladder cancer diagnosis, Biosens. Bioelectron. 79 (2016) 789–795. https://doi.org/10.1016/j.bios.2016.01.005.

[133] J. de Cássia Mendonça, L.R. da Rocha, T.B. Capelari, M.C. Prete, P.N. Angelis, M.G. Segatelli, C.R.T. Tarley, Design and performance of novel molecularly imprinted biomimetic adsorbent for preconcentration of prostate cancer biomarker coupled to electrochemical determination by using multi-walled carbon nanotubes/Nafion®/Ni(OH)2-modified screen-printed electrode, J. Electroanal. Chem. 878 (2020) 114582. https://doi.org/10.1016/j.jelechem.2020.114582.

[134] Y. Wu, Y. Wang, X. Wang, C. Wang, C. Li, Z. Wang, Electrochemical Sensing of α-Fetoprotein Based on Molecularly Imprinted Polymerized Ionic Liquid Film on a Gold Nanoparticle Modified Electrode Surface, Sensors. 19 (2019) 3218. https://doi.org/10.3390/s19143218.

[135] O. Sheydaei, H. Khajehsharifi, H.R. Rajabi, Rapid and selective diagnose of Sarcosine in urine samples as prostate cancer biomarker by mesoporous imprinted polymeric nanobeads modified electrode, Sens. Actuators B Chem. 309 (2020) 127559. https://doi.org/10.1016/j.snb.2019.127559.

[136] M. Pirzada, E. Sehit, Z. Altintas, Cancer biomarker detection in human serum samples using nanoparticle decorated epitope-mediated hybrid MIP, Biosens. Bioelectron. 166 (2020) 112464. https://doi.org/10.1016/j.bios.2020.112464.

[137] J. Li, X. Ma, M. Li, Y. Zhang, Does polysaccharide is an idea template selection for glycosyl imprinting?, Biosens. Bioelectron. 99 (2018) 438–442. https://doi.org/10.1016/j.bios.2017.08.004.

[138] M. You, S. Yang, W. Tang, F. Zhang, P. He, Molecularly imprinted polymers-based electrochemical DNA biosensor for the determination of BRCA-1 amplified by SiO2@Ag, Biosens. Bioelectron. 112 (2018) 72–78. https://doi.org/10.1016/j.bios.2018.04.038.

[139] X. Shen, Y. Ma, Q. Zeng, J. Tao, J. Huang, L. Wang, Molecularly imprinted electrochemical sensor for advanced diagnosis of alpha-fetoprotein, Anal. Methods. 8 (2016) 7361–7368. https://doi.org/10.1039/C6AY01922F.

[140] G. Zhang, Y. Yu, L. Zhang, B. Lin, Y. Wang, M. Guo, Y. Cao, Precise detection of prostate specific antigen in serum: A surface molecular imprinted sensor based on novel cooperated signal amplification strategy, Sens. Actuators B Chem. 302 (2020) 126998. https://doi.org/10.1016/j.snb.2019.126998.

[141] A.E.F. Oliveira, A.C. Pereira, L.F. Ferreira, Disposable electropolymerized molecularly imprinted electrochemical sensor for determination of breast cancer biomarker CA 15-3 in human serum samples, Talanta. 252 (2023) 123819. https://doi.org/10.1016/j.talanta.2022.123819.

[142] F. Ben Moussa, C. Ait-Ramdane-Terbouche, A. Terbouche, H. Belkhalfa, D. Guerniche, A. Zouaoui, Novel thermal synthesis of ternary Cu-CuO-Cu2O nanospheres supported on reduced graphene oxide for the sensitive non-enzymatic electrochemical detection of pyruvic acid as a cancer biomarker, J. Organomet. Chem. 989 (2023) 122638. https://doi.org/10.1016/j.jorganchem.2023.122638.

[143] G.K. Ali, K.M. Omer, Molecular imprinted polymer combined with aptamer (MIP-aptamer) as a hybrid dual recognition element for bio(chemical) sensing applications. Review, Talanta. 236 (2022) 122878. https://doi.org/10.1016/j.talanta.2021.122878.